

Economic valuation of subsurface water contributions to watershed ecosystem services using a fully-integrated groundwater–surface water model

Tariq Aziz^{1,2,*}, Steven K. Frey^{1,3}, David R. Lapen⁴, Susan Preston⁵, Hazen A. J. Russell⁶, Omar Khader^{1,7}, Andre R. Erler¹, Edward A. Sudicky^{1,3}

¹Aquanty, 600 Weber St. N., Unit B, Waterloo, ON, N2V 1K4, Canada

²Ecohydrology Research Group, Water Institute and Department of Earth and Environmental Sciences, University of Waterloo, Waterloo, N2L 3G1, ON, Canada

³Department of Earth and Environmental Sciences, University of Waterloo, Waterloo, N2L 3G1, ON, Canada

⁴Agriculture and Agri-Food Canada, Ottawa Research and Development Centre, Ottawa, Ontario, Canada

⁵Environment and Climate Change Canada, Ottawa, Ontario, Canada

⁶Geological Survey of Canada, 601 Booth St., Ottawa, ON, K1A 0E8, Canada

⁷Department of Water and Water Structural Engineering, Zagazig University, AlSharqia, Egypt

*Correspondence to: Tariq Aziz (taziz@aquanty.com)

Abstract. Water is essential for all ecosystem services, yet a comprehensive assessment and valuation of total (overall) water contributions to ecosystem services production has never been attempted. Quantification of the many ecosystem services impacted by water demands an analytical approach that implicitly characterizes both subsurface and surface water resources; however, incorporating subsurface water into ecosystem services evaluation has until now remained elusive. In this study, a fully-integrated groundwater–surface water model—HydroGeoSphere (HGS)— is used to capture changes in subsurface water, surface water, and transpiration (green water use), and along with an economic valuation approach, forms the basis of an ecosystem services assessment for an 18-year period (2000-2017) in a mixed-use but a predominantly agricultural watershed in eastern Ontario, Canada. Using green water volumes generated by HGS and ecosystem services values as inputs, the marginal productivity of water is calculated to be \$0.26 per m³ (in 2022 Canadian dollars). Results show maximum green water values during the driest years, with the extreme drought of 2012 being the highest at \$424.7 million. In contrast, the green water value in wetter years was as low as \$245.9 million, while the 18-year average was \$338.83 million. Because subsurface water is the sole contributor to the green water supply it plays a critical role in sustaining ecosystem services during drought conditions. This study provides new insight into the economic contributions of subsurface water and its role in sustaining ecosystem services during droughts, and puts forth improved methodology for watershed-based integrated management and valuation of ecosystem services.

1 Introduction

The role of subsurface water (groundwater and soil water in the vadose zone) in socio-economic development is widely acknowledged (Foster and Chilton, 2003); however, its ecological contributions are undervalued (Yang and Liu, 2020), despite being fundamental to the control of terrestrial ecological processes (Qiu et al., 2019). Subsurface water supports a potpourri of ecosystem services that range from provisioning to regulating, supporting, and cultural

36 services (Griebler and Avramov, 2015). While infiltration is a driver for subsurface water recharge, subsurface water
37 discharge is in-turn key for supporting terrestrial ecosystems (e.g., wetlands, forests, etc.) (Griebler and Avramov,
38 2015). Subsurface water provides a buffer against weather stressors on vegetation and aquatic ecosystems and helps
39 to maintain key processes that underpin ecosystem services (Qiu et al., 2019). To date, most ecosystem services
40 research has focused on aboveground factors and processes (e.g., land use change), and very little focus has been given
41 to the critical zone (e.g., shallow groundwater) and its influence on terrestrial ecosystem services (Richardson and
42 Kumar, 2017; Qiu et al., 2019). While some previous research (e.g., Booth et al., 2016; Li et al., 2014) has attempted
43 to link subsurface water with land cover, it reflects field scale, static environmental conditions (Qiu et al., 2019).
44 Given the difficulties with mapping large/watershed scale subsurface water resources, the contribution of subsurface
45 water towards terrestrial ecosystem services is not typically quantified, and the monetary/economic valuation of
46 subsurface water contribution to terrestrial ecosystem services is overlooked.

47 While hydrologic ecosystem services studies are common in the literature (Ochoa and Urbina-Cardona, 2017),
48 groundwater-focused ecosystem services assessments are rare. However, groundwater can be an important regulator
49 of watershed hydrologic behaviour and ecosystem health, especially in regions with a shallow water table, such as the
50 Laurentian Great Lakes Region (Neff et al., 2005; Kornelsen and Coulibaly, 2014). In addition, groundwater acts as
51 a source of soil water in shallow water table areas (Chen and Hu, 2004). The importance of groundwater has been
52 noted by Griebler and Avramov (2015) in their review of groundwater ecosystem services, where they highlight the
53 direct role it plays in supplying different types of ecosystem services (Millenium Ecosystem Assessment (MEA),
54 2005); and they stress the need for a better quantitative understanding of groundwater processes in order to protect
55 and manage groundwater ecosystem services. Furthermore, Mammola et al. (2019) emphasize that subterranean
56 ecosystems are largely being overlooked in conservation policies. Based on a preliminary assessment of all the regions
57 around the world where groundwater plays a critical role in ecosystem services, and considering that approximately
58 43 % of consumptive irrigation is sourced from groundwater (Siebert et al., 2010), one has to wonder if the lack of
59 focus on subsurface water ecosystem services is not due to lack of need, but in fact a lack of tools with which to
60 conduct the required analysis.

61 Hydrological models provide a convenient approach for characterizing water storages and fluxes over large spatial
62 scales. With groundwater ecosystem services' increasing role in policy-making (Honeck et al., 2021) and sustainable
63 groundwater resources management, new tools are required for the mapping process. At present, common modeling

64 tools available for ecosystem services mapping include relatively simple matrix models (i.e., Decsi et al., 2022), and
65 more complex models such as ARTificial Intelligence for Environment & Sustainability (ARIES) (Villa et al., 2021),
66 Co\$ting Nature (Mulligan, 2015), Envision (Bolte, 2022), and Integrated Valuation of Ecosystem Services and
67 Tradeoffs (InVEST) (Natural Capital Project, 2022), with InVEST being by far the most prominent in the scientific
68 literature (Ochoa and Urbina-Cardona, 2017). However, ecosystem services specific models, such as the InVEST
69 Water Yield Model, have limited capability to simulate hydrological processes efficiently (Redhead et al. 2016),
70 because their hydrologic tools typically focus on one water compartment and/or are simplified to the point where
71 hydrologically mediated ecosystem services cannot be fully characterized (Dennedy-Frank et al., 2016; Vigerstol and
72 Aukema, 2011). Complete characterization of spatially and temporally varying water storages and fluxes that govern
73 ecosystem services over large spatial scales requires more sophisticated, process-based hydrological models (Sun et
74 al., 2017). Hence, models like SWAT (Arnold et al., 1998) and the Variable Infiltration Capacity (VIC) model (Liang
75 et al., 1994) have been used for hydrologic ecosystem services assessment, however even these models are unable to
76 simulate complex subsurface water movement and water exchanges between the surface and subsurface. Within the
77 hydrologic modelling community, it is acknowledged that structurally complex, fully-integrated subsurface–surface
78 water models are the current state-of-the-art for capturing the interplay between subsurface and surface water systems
79 (Barthel and Banzhaf, 2016; Berg and Sudicky, 2019), however, this class of models has not yet been applied towards
80 ecosystem services valuation.

81 A key hydrologic process influencing ecosystem services is evapotranspiration, which can be closely related to the
82 availability of shallow groundwater (Jin et al., 2017; Condon et al., 2020). Evapotranspiration is a fraction of rainfall
83 that eventually returns to the atmosphere through evaporation and transpiration, which represent large fluxes of both
84 water and energy across the land surface–atmosphere boundary (Tan et al., 2021). While evaporation is often perceived
85 as a water loss, transpiration is an essential process for sustaining ecosystems and providing terrestrial ecosystem
86 services (An and Verhoeven, 2019). Transpiration is also called productive green water—the fraction of the rainfall
87 on the land that eventually returns to the atmosphere via plants. It is a source of nutrition for vegetation/ecosystems
88 (Casagrande et al., 2021), and plays a key role in the production of biomass and ecosystem services (Zisopoulou et
89 al., 2022; Schyns et al., 2019). Green water is essential for functioning and growth of ecosystems, and thus supports
90 and maintains terrestrial ecosystem services (Lowe et al., 2022). Hence, transpiration serves as a key driver in

91 providing ecosystem services (Liu and El-Kassaby, 2017), and is a fundamental process by which to model/map
92 terrestrial ecosystem services production.

93 Changes in evapotranspiration rates can influence water availability and ecosystem health at a watershed scale (Zhao
94 et al., 2022). Thus, subsurface water availability is an important when considering ecosystem function and ecosystem
95 services. Under drought conditions, subsurface water can become critically important for sustaining transpiration
96 (Condon et al., 2020), and hence, mapping the subsurface water - transpiration connection is imperative for sustainable
97 water and ecosystem services management (Yang et al., 2015). In cases where growing climate variability is expected
98 to result in increasingly erratic precipitation patterns, capturing these connections becomes even more important
99 (Taylor et al., 2013). While a few common hydrological models can weakly capture the subsurface water dynamics
100 and subsurface-surface water interactions (Clark et al., 2015), fully integrated subsurface-surface hydrologic models
101 can dynamically resolve water exchange between groundwater, surface water, and soil moisture, and evaporation and
102 transpiration fluxes with much higher levels of spatial and temporal fidelity. Benchmarking studies have been
103 conducted wherein the most common subsurface-surface hydrologic models have been described in detail, and their
104 simulation behavior compared (Maxwell et al., 2014; Kollet et al., 2016).

105 In this study, we introduce the HydroGeoSphere (HGS) fully-integrated subsurface-surface water model (Aquanty,
106 2021; Brunner and Simmons, 2012) as a tool for mapping key hydrological fluxes and water storage fluctuations, and
107 quantifying subsurface water contributions to terrestrial ecosystem services at the watershed scale (~4000 km²). The
108 results from the HGS modelling are extended to an economic valuation of water contributions to ecosystem services.
109 Until now, fully-integrated subsurface-surface models such as HGS have not been widely demonstrated in the
110 scientific literature as tools for modeling ecosystem services, while at the same time, the economic value of subsurface
111 water has been overlooked in ecosystem services valuation assessments. Accordingly, the study herein is a novel
112 contribution towards improving our understanding of overall hydrologic contributions to ecosystem services.
113 Furthermore, using the HGS model outputs to support the economic valuation of subsurface water contributions to
114 transpiration, and subsequently to terrestrial ecosystem services, is also novel. Hence, this work provides an important
115 advancement to the science of ecosystem service valuation in terms of conceptual, methodological, and quantitative
116 understanding.

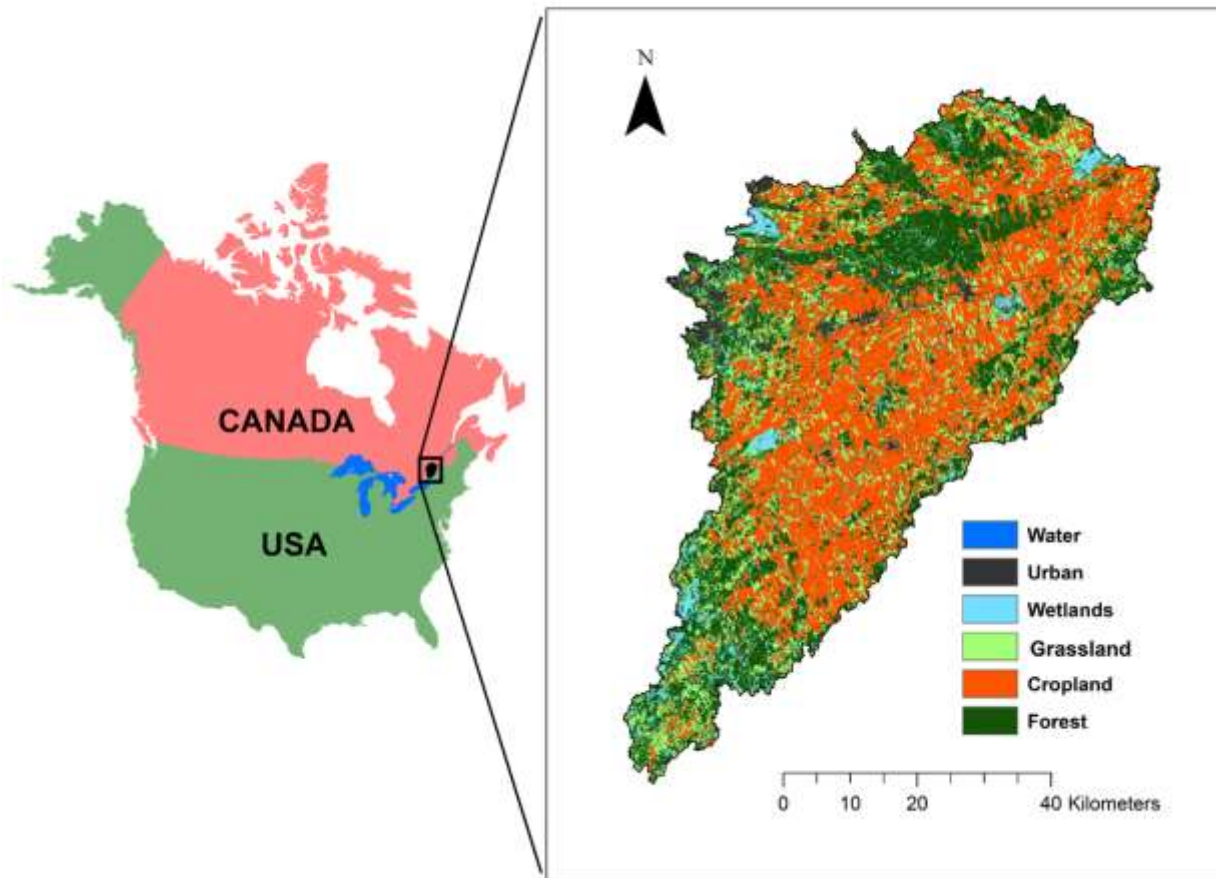
117 **2 Materials and Methods**

118 **2.1 Study Area**

119 This study focuses on the South Nation watershed (SNW), located in eastern Ontario, Canada, with an area of
120 approximately 3,830 km² (Fig. 1). The SNW is relatively flat, with approximately 100 m of vertical relief in the land
121 surface. It is primarily an agriculture-focused watershed, with relatively low population density, where for example
122 the towns of Casselman, Russell, and Winchester (population centres within the SNW) have respective populations
123 of 3,548, 16,520 and 2,394 based on the 2016 Canada census. The eastern flank of the city of Ottawa encroaches on
124 the Northwest corner of the watershed. The SNW surface water flow network is approximately 6,489 km long and
125 consists of 1,606 km of Strahler order 3+ (relatively large), 1,548 km of Strahler order 2, and 3,335 km of Strahler
126 order 1 (smallest) river and stream features (Fig. 2A). Many of the low order features are either manmade agricultural
127 drainage ditches or straightened natural watercourses designed to drain the agricultural landscape.

128 Soil drainage conditions across the watershed are primarily imperfect, poor, or very poor (Fig. 3A), although some
129 disconnected pockets are considered well drained (Soil Landscapes of Canada Working Group, 2010). The wide extent
130 of poorly drained soils in the SNW is an integral reason for the intensive land drainage activities. Tile drainage is
131 employed in approximately 960 km² (or 25 %) of the watershed to enhance agricultural productivity and to facilitate
132 cropping activities (Fig. 4A). Across most of the SNW the soils are primarily underlain by glacial, fluvial, and colluvial
133 Quaternary deposits (Ontario Geological Survey, 2010). These sediments are composed of sand, silt, clay, gravel, and
134 glacial till, and range in thickness from 0 m to approximately 90 m across the watershed. Eight soils have been
135 identified in the SNW (Soil Landscapes of Canada Working Group, 2010), mainly composed of clay loam and sandy
136 loam textures (Fig. 3A(a)). Localized incised bedrock channels and Quaternary esker deposits are important sources
137 of groundwater for both ecological function and human/livestock supply, and most of the rural residents in the SNW
138 rely on groundwater for domestic and farm use.

139 The SNW is characterized by relatively wet temperate climate with cold winters and warm summers. The annual
140 average temperature is just over 5 C, with average summer highs reaching 26°C in July and average winter lows
141 reaching -14°C in January (https://climate.weather.gc.ca/climate_normals). Present day landcover (Fig. 1) consists of
142 38% cropland, 29% forest, 20% grassland, 7% urban, 5% wetland, and 1% water. Within the SNW, grasslands support
143 the extensive dairy industry, which plays an important role in the local economy.



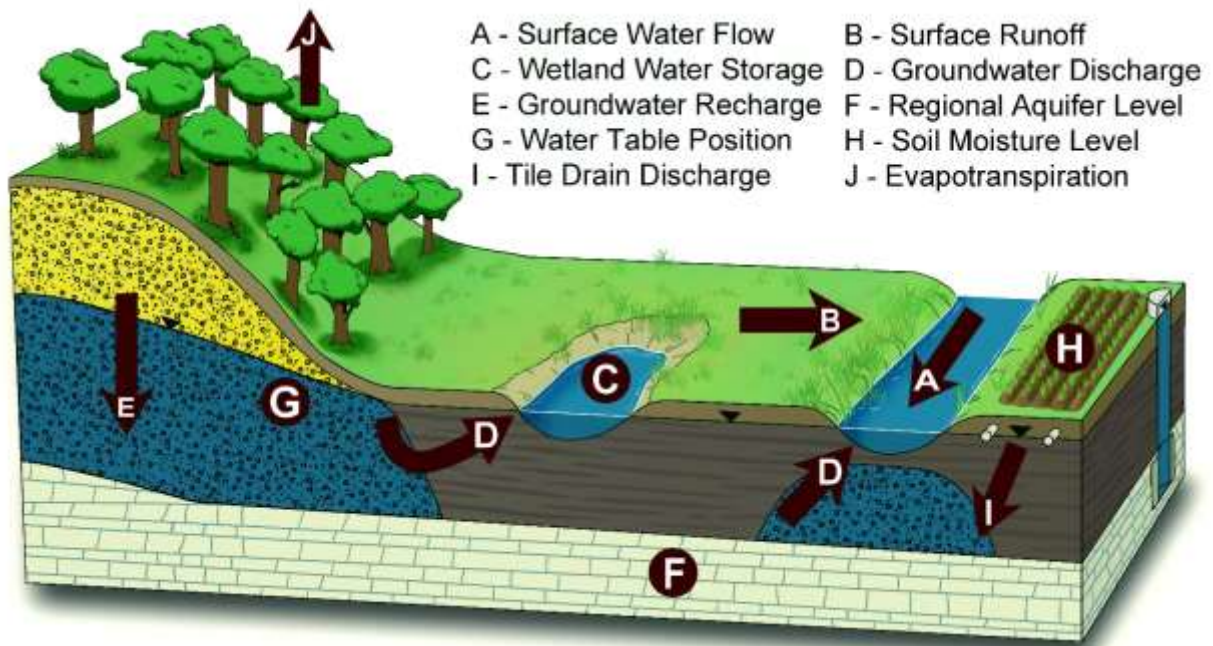
144

145 **Figure 1: Location of the South Nation Watershed (SNW) in North America. The inset figure (right) shows the**
 146 **land use distribution across the SNW.**

147 **2.2 Water balance quantification with HydroGeoSphere (HGS)**

148 The water balance strongly influences ecosystem functions and the associated ecosystem services, as it governs both
 149 abiotic and biotic processes occurring within ecosystems (Mercado-bettín et al., 2019). Consequently, evaluating the
 150 role of water towards ecosystem services supply necessitates an analysis capable of water balance partitioning (i.e.,
 151 disaggregation of the water balance into its fundamental components such as precipitation, subsurface evaporation,
 152 transpiration, surface and subsurface storages) (Casagrande et al., 2021). As HGS is a dynamic fully-integrated
 153 subsurface–surface hydrologic model, it generates time varying simulation outputs for all components of the terrestrial
 154 hydrologic cycle (Fig. 2), thus alleviating a common limitation of ecosystem services models in that they do not
 155 account for transient behavior (Vigerstol and Aukema, 2011). HGS employs a physically based approach to simulate

156 water movement and the partitioning of precipitation input into surface runoff, streamflow, evaporation, transpiration,
157 groundwater recharge, as well as groundwater discharge into surface water bodies like rivers and lakes (Brunner and
158 Simmons, 2012). Furthermore, HGS outputs can also be generated for the entire model domain (i.e., the watershed)
159 or refined for smaller spatial scales such as subwatersheds, with the downscale limit being that of an individual finite
160 element within the finite element mesh (FEM).



161
162 **Figure 2: Key components of the terrestrial hydrological cycle captured in HGS models over a range of spatial**
163 **scales.**

164 It should be noted that the fidelity of the HGS outputs are also dependent on the model scale, with large scale models
165 generally having lower spatial resolution than small scale models as a result of computational constraints, and in some
166 cases, data constraints. For example, a model of a 766,000 km² river basin (e.g., Xu et al., 2021a)) is best suited to
167 answer big picture questions (i.e., basin water balance, regional groundwater), while a model built at similar scale to
168 the SNW (e.g., Frey et al., 2021)) can be used to address questions pertaining to localized processes (i.e., individual
169 wetland influences, groundwater recharge and discharge patterns, aquifer conditions, and soil moisture conditions). If
170 even more localized insights are required, HGS models can be constructed for field or plot scale domains (up to
171 approximately 10 km²), where highly detailed questions pertaining to things such as riparian zones, soil structure,
172 manure application, and tile drainage influences on both water quantity and quality can be evaluated (Fig. 2). Thus,

173 HGS is a scalable and robust model for ecosystem services analysis across a range of different spatial scales and
174 different levels of hydrologic process detail. For the SNW, HGS is used to simulate watershed surface water outflow,
175 transpiration (green water), subsurface water storage, and land surface water storage (reflecting water held in wetlands
176 and reservoirs) using the model construction framework presented in Frey et al. (2021).

177 **2.2.1 Model construction**

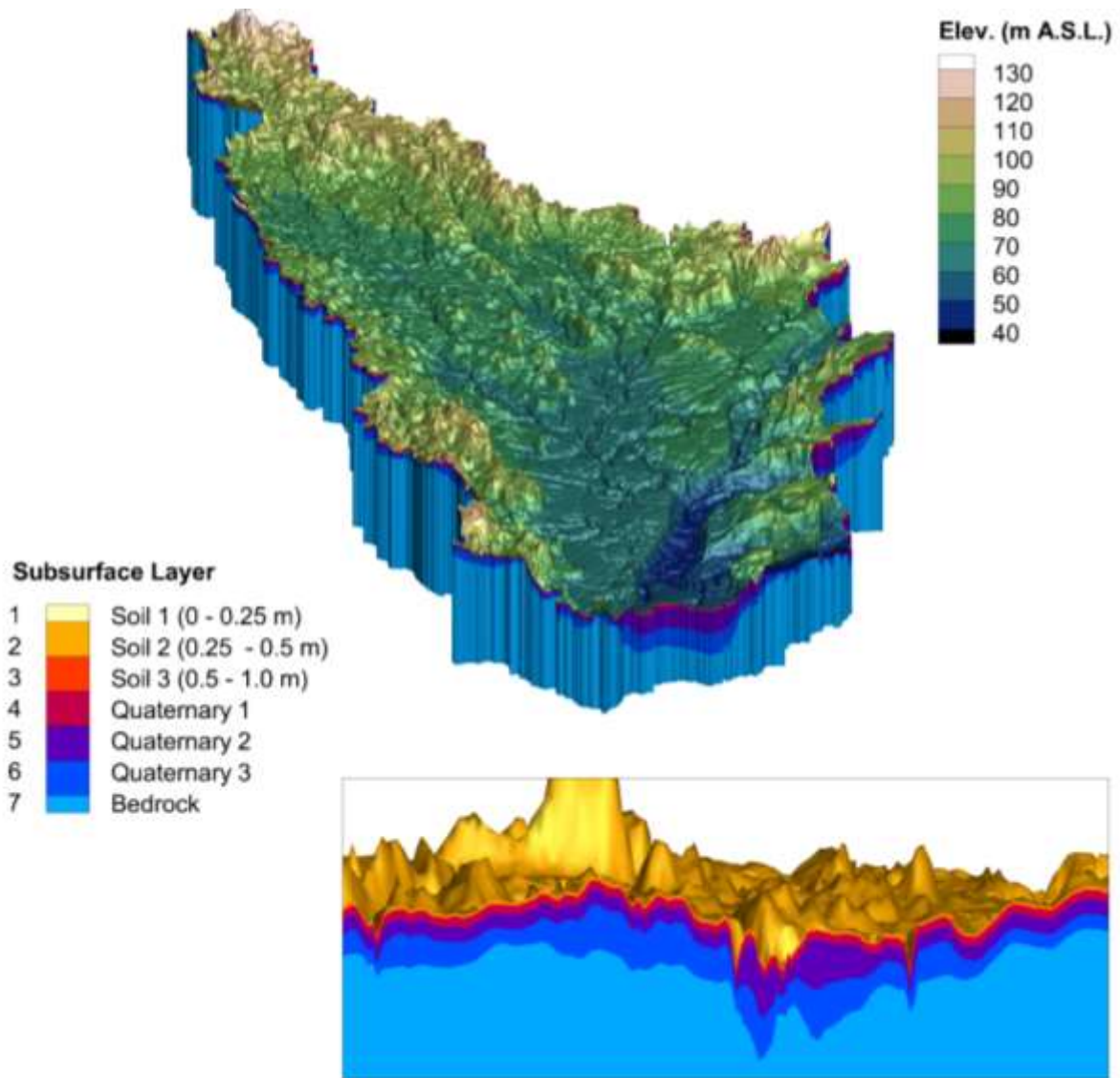
178 **2.2.1.1 Finite Element Mesh (FEM)**

179 The HGS model utilizes a 3-D unstructured FEM that extends across the full 3830 km² area of the SNW. The 1-D
180 river/stream channel features, 2-D overland flow domain (reflecting land surface topography), and 3-D subsurface
181 flow domain (reflecting hydrostratigraphy) all share the same mesh geometry, with the 1-D and 2-D domains sharing
182 common coordinates with the 3-D domain across the top surface of the model. The FEM for the SNW model resolves
183 all Strahler 2+ stream/river features as mesh discretization control lines, with element edge length maintained at 100
184 m, while away from the control lines the element edge lengths extend up to 300 m. The FEM contains layer surfaces
185 that correspond to hydrostratigraphic surfaces, with each individual layer consisting of 171,609 finite elements.
186 Accordingly, over the eight model surfaces (seven subsurface layers); the FEM contains 1,201,263 3-D finite elements.

187 **2.2.1.2 Hydrostratigraphy**

188 The seven subsurface layers represent (from the top down) three soil layers, three Quaternary hydrostratigraphic
189 layers, and one bedrock layer. The soil layers extend from 0–0.25 m, 0.25–0.5 m, and 0.5–1 m depth relative to the
190 top surface, which is defined with the Ontario Integrated Hydrology Data digital elevation model
191 (<https://geohub.lio.gov.on.ca/maps/mnrf::ontario-integrated-hydrology-oih-data/about>). The hydraulic properties for
192 the soil layers vary spatially according to the soil polygons defined in the Soil Landscapes of Canada (SLC, Soil
193 Landscapes of Canada Working Group, 2010), and are defined in two steps as follows: (1) properties extracted from
194 SLC are used in conjunction with the Rosetta pedotransfer functions (Schaap et al., 2001) to obtain estimates for
195 hydraulic conductivity, water retention and relative permeability, residual saturation, and porosity parameters, and (2)
196 hydraulic conductivity, water retention and relative permeability parameters are subsequently tuned during model
197 calibration. The three Quaternary layers are of variable thickness, where the interface surfaces represent lithology
198 contrasts derived from a simplified version of the 3-D geological model produced for the SNW by Logan et al. (2009).
199 Hydraulic properties for the Quaternary materials are assigned based on lithology. Underlying the Quaternary layers

200 is a single hydrostratigraphic layer with uniform hydraulic conductivity representative of the Phanerozoic bedrock.
201 When assembled, the model layers depict a 3-D subsurface realization of the SNW hydrostratigraphy (Fig. 3).



202
203 **Figure 3: Three-dimensional perspective of the South Nation HydroGeoSphere model, and the**
204 **hydrostratigraphic layering (inset). Note the 100x vertical exaggeration.**

205 2.2.1.3 Land Surface Configuration

206 The land surface in the HGS model represents land cover distribution defined by the gridded, 30 m resolution, 2017
207 Annual Crop Inventory dataset (Agriculture and Agri-Food Canada, 2022) simplified to six categories (water, urban,
208 wetland, grassland, cropland, and forest). Root depth for the cropland (1 m), forest (2.9 m), wetland (1 m), grassland
209 (2.1 m), and urban (1 m) landcovers was held static over the simulation interval. Spatially distributed leaf area index
210 (LAI) is a transient parameter defined with the 8-day composite, 500 m resolution MOD15A2H v006 data product

211 (Myneni et al., 2021). Each landcover category utilizes a unique surface roughness (Manning's n coefficient) value,
212 ranging from 0.001 (urban) to 0.03 $s/m^{1/3}$ (forest). Land cover properties, as well as subsurface hydraulic properties,
213 were mapped into the HGS model's unstructured FEM using a dominant component approach, such that when two or
214 more property classes exist within the input data set for a single finite element, the majority class is represented.

215 **2.2.1.4 Climatology**

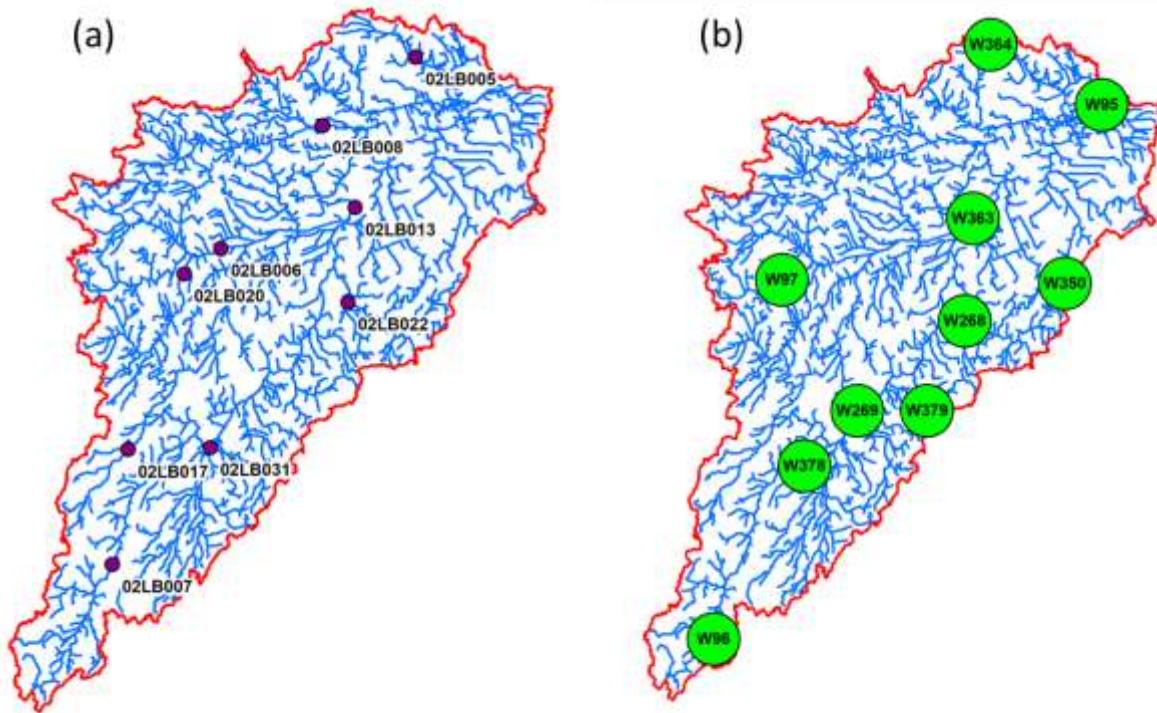
216 Time-varying and spatially distributed climate data with daily temporal resolution liquid water influx (LWF) and
217 potential evapotranspiration (PET) is used to force the HGS model for the 2000 to 2018 simulation interval. LWF is
218 derived from precipitation obtained from McKenney et al. (2011) in combination with snow water equivalent (SWE)
219 estimates from the ERA5-Land land-surface reanalysis (Muñoz-Sabater et al., 2021), where LWF is the sum of liquid
220 precipitation (rain) and snowmelt (daily changes in SWE).

221 Potential evapotranspiration primarily depends on the surface radiation budget, temperature, humidity, and near-
222 surface wind speed (Allen et al., 1998); however, of these variables, only minimum and maximum temperature are
223 readily available for the full SNW. Hence, PET forcing for the SNW model is calculated with the Hogg method (Hogg,
224 1997), which is consistent with Erler et al. (2019) and Xu et al. (2021), who both reported good agreement with the
225 observed water balance in the Great Lakes region when using the Hogg method. The Hogg method is based on the
226 FAO Penman-Monteith approach (Allen et al. 1998) with a simplification that involves the radiation budget and
227 humidity approximated as a function of daily minimum and maximum temperature, and wind speed assumed to be
228 constant.

229 **2.2.2 Model Performance Evaluation**

230 The SNW HGS model was run continuously for the 2000–2017 with daily temporal resolution climate forcing, and
231 simulation performance is evaluated using observed surface water flow rates and groundwater levels. The observation
232 data is derived from daily temporal resolution surface water flow monitoring conducted at nine Water Survey of
233 Canada (WSC) hydrometric stations (Figure 4a) and groundwater level data from 10 Provincial Groundwater
234 Monitoring Network wells that was collected hourly but aggregated into daily average values (Figure 4b). The Nash-
235 Sutcliffe Efficiency (NSE) and Percent Bias (Pbias) metrics (Moriasi et al., 2007) are used to evaluate surface water
236 flow simulation performance, while the coefficient of determination (R^2) and root mean square error (RMSE) is used
237 to evaluate groundwater simulation performance. It should be noted that groundwater pumping is not represented in

238 the model as it is deemed to be a very minor component of the overall water balance, and because it is extremely
239 difficult to characterize and simulate at the scale of the SNW.



240
241 **Figure 4: Distribution of (a) Water Survey of Canada surface water flow gauges, and (b) Provincial**
242 **Groundwater Monitoring Network wells across the South Nation watershed.**

243 2.3 Ecosystem services water productivity

244 The benefit transfer method is used to derive the unit values of ecosystems in the SNW. The benefit transfer method,
245 which is a widely used technique for assessing the economic value of ecosystem services, relies on secondary data
246 obtained through the implementation of various other economic valuation methods (Aziz, 2021). A study conducted
247 approximately 65 km from the SNW in the Ottawa-Gatineau region, by L'Ecuyer-Sauvageau et al. (2021), assembles
248 the values for 13 ecosystem services: agricultural services, global climate regulation, air quality, water provision,
249 waste treatment, erosion control, pollination, habitat for biodiversity, natural hazard prevention, pest management,
250 nutrient cycling, landscape aesthetics, and recreational activities. Because of data limitations, raw material, genetic
251 diversity, spiritual, cultural and heritage identity ecosystem services are excluded from the L'Ecuyer-Sauvageau et al.
252 (2021) analysis. These unit values have been correspondingly generated by major ecosystems using market price,
253 replacement cost, and benefit transfer methods. The unit values for ecosystem services are based on similarities in

254 ecologic and socio-economic conditions between the studied and policy sites, and converted using the purchasing
 255 power parity (L'Ecuyer-Sauvageau et al., 2021). After adjusting these values for inflation, the value of ecosystem
 256 services in the SNW is calculated using the following equation.

$$257 \quad EV_t = \sum_{k=1}^n (A_k \times UV_k) * VI \quad (1)$$

258 EV_t = Value of ecosystem services for year t

259 A_k = Area of land use k

260 UV_k = Unit value of ecosystem services for land use k

261 VI = Vegetation indicator, a ratio of yearly to average net primary production (NPP) = NPP_{year}/NPP_{mean}

262 We use net primary production as an indicator to characterize the vegetation vigor (Xu et al., 2012) and to adjust the
 263 values of ecosystem services over time in the SNW. The relative vegetation indicator (VI) is the ratio of yearly NPP
 264 and the mean NPP over the selected period. The Moderate Resolution Imaging Spectroradiometer (MODIS)
 265 (<https://appears.earthdatacloud.nasa.gov/>) NPP data (at 500m resolution) for the 2000 to 2017 study period is used.
 266 Using the ArcGIS Spatial Analyst Toolbox, yearly mean NPP values are calculated (Table 2). The average ecosystem
 267 services water productivity is then calculated using ecosystem services values and productive green water volumes
 268 (i.e., transpiration) in equation 2:

$$269 \quad V_w = (EV_t)/(X_w) \quad (2)$$

270 V_w is the average product of water (\$ per m³), X_w is the total volume of water transpired (or productive green water
 271 volume) in a year 't'.

272 **2.4 Valuation of subsurface water contribution towards ecosystem services supply**

273 A water production function is developed using economic values of the watershed for ecosystem services supply over
 274 the 18-year study period and corresponding volumes of green water consumption. Because ecosystem services value
 275 is proportional to biomass production (Costanza et al., 1998), the values are modified over time using relative changes
 276 in ecosystems biomass in the watershed (Xu and Xiao, 2022). The slope of the production function represents the
 277 ecosystem services marginal water productivity (MP_w). HGS model outputs capture the volume of subsurface water
 278 contributing to transpiration. Using the volumes of subsurface water consumed for transpiration and MP_w , the
 279 economic value of green water from the storages used for ecosystem services supply is calculated (Eq.3).

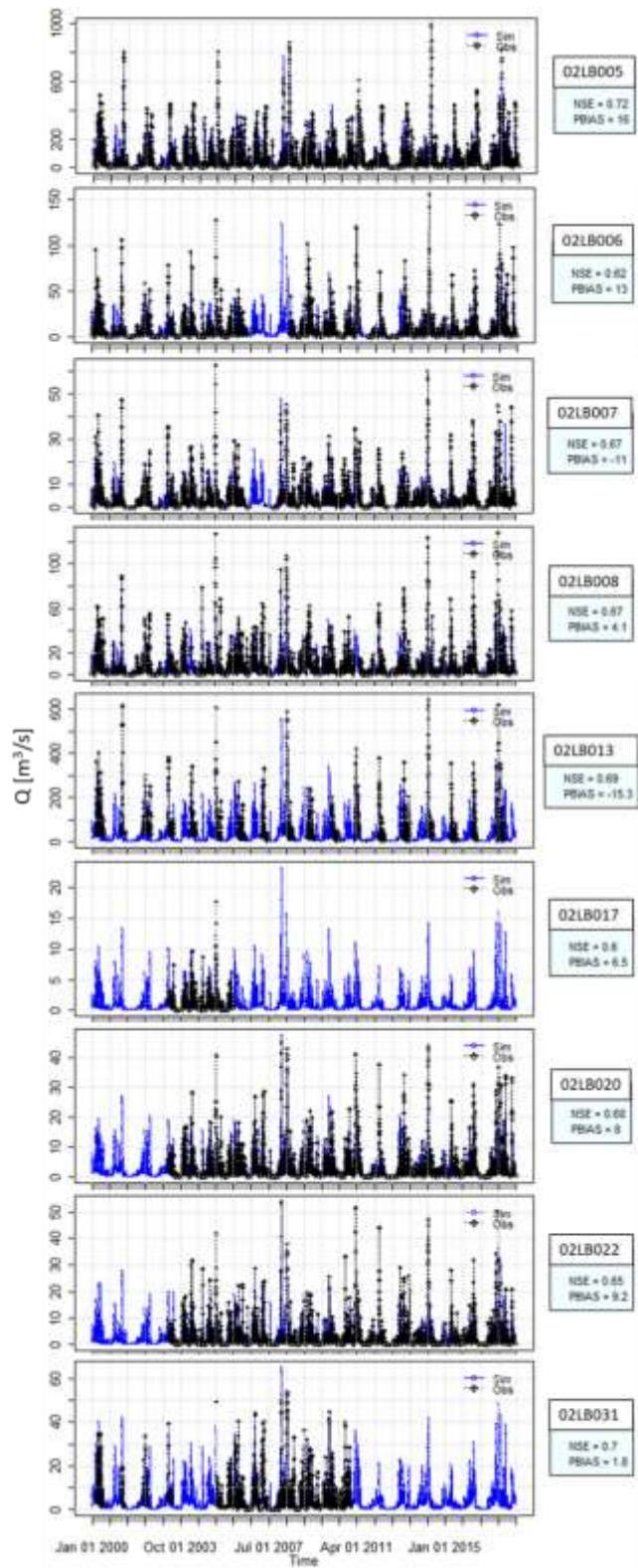
$$280 \quad V_i = X_{wi} * MP_w \quad (3)$$

281 Where V_i is the value of water storage i towards ecosystem services supply, X_{wi} is the volume of water storage i used
282 towards green water supply, and MP_w is the marginal productivity of water.

283 **3 Results**

284 **3.1 HGS outputs**

285 For the 2000 to 2017 simulation interval, the HGS model reproduces surface water flow rates at the nine WSC
286 hydrometric stations across the SNW with good accuracy per the interpretation guidance provided by Moriasi et al.
287 (2007). Based on daily evaluation frequency, NSE at the individual gauge stations ranges from 0.59 to 0.70, with a
288 mean of 0.66; while PBias ranged from -17.4 % to 17.1 %, with a mean of 3.9 % (Fig. 5). Groundwater levels were
289 also reproduced across the SNW with reasonable accuracy for the 2000 to 2017 interval. The R^2 between simulated
290 and observed water levels in the 10 observation wells is 0.98, with the simulated values having a mean value 2.8 m
291 higher than the observed values. Groundwater simulation performance at the individual wells is presented in Table 1.
292 HGS outputs (Fig. 6) also include total watershed surface water outflow, ET_a rates (based on subsurface transpiration
293 and evaporation, surface evaporation and canopy evaporation), subsurface water storage (groundwater storage plus
294 soil moisture storage) and land surface water storage. During the simulation period, transpiration accounts for a
295 substantial proportion of ET_a , ranging from 45% to 65% (Table A1). Consequently, it emerges as the dominant process
296 contributing to the overall ET_a . As evident in Fig. 6, water storage volumes fluctuate over inter- and intra-annual time
297 frames, with the most notable decline in storage aligned closely with the drought in 2012.



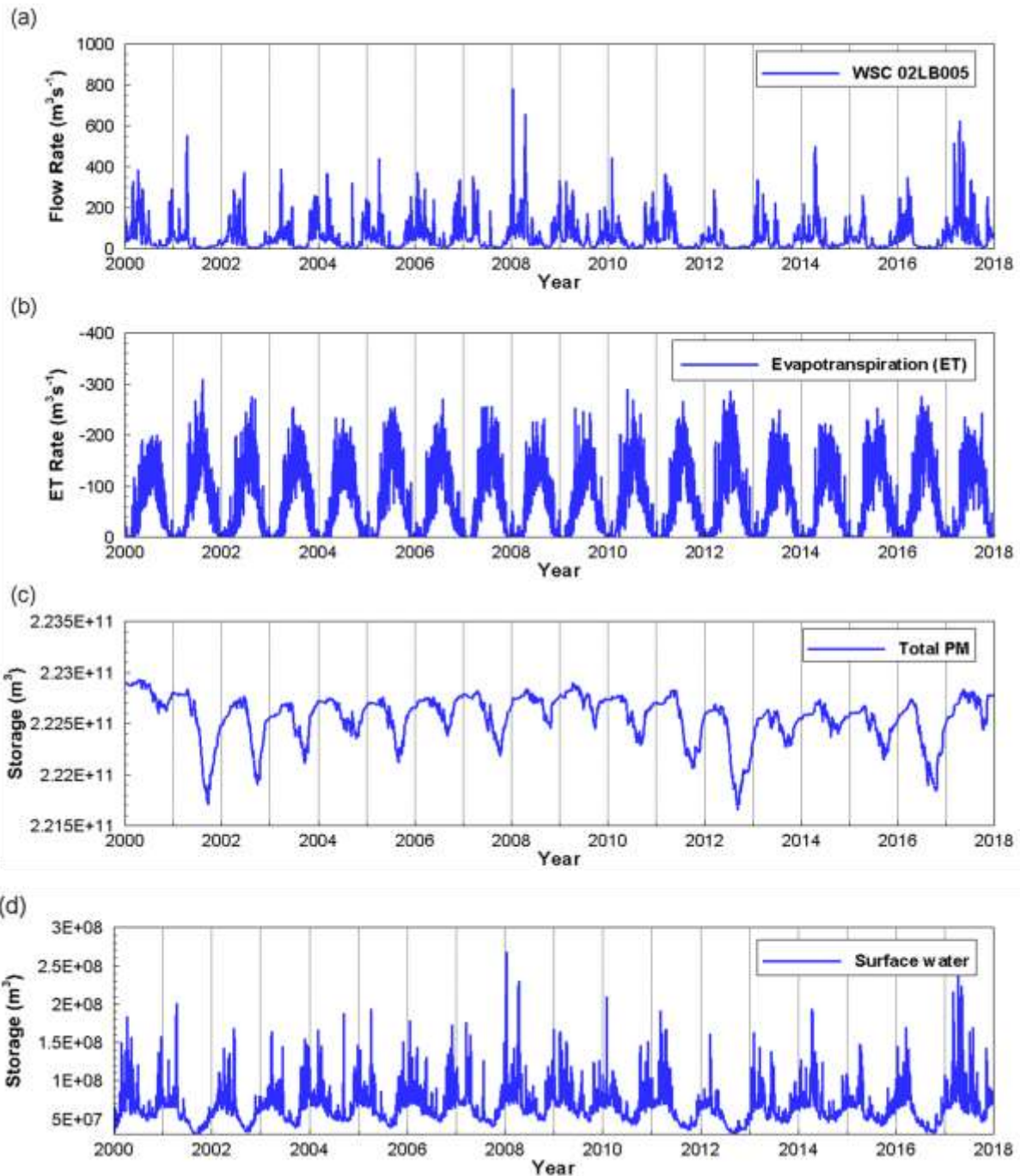
298

299 Figure 5: Simulated vs. observed surface water flow rates at the nine Water Survey of Canada (WSC) flow gauges
 300 incorporated into the model calibration process, along with Nash-Sutcliffe Model Efficiency (NSE) and Percent Bias (PBias
 301 in %) performance metrics. Note that not all gauges have a full data record over the 18-year simulation interval.

302 **Table 1. For the 10 monitoring well locations, observed vs. simulated average groundwater head, and root mean square**
 303 **error between daily temporal resolution observed and simulated head, over the 2000 – 2017 simulation interval.**

Well	Observed Average Head (mASL)	Simulated Average Head (mASL)	RMSE (m)
95	48.2	62.0	13.8
96	99.1	99.1	0.8
97	84.9	86.9	2.1
268	72.4	72.3	0.5
269	68.4	70.9	2.7
350	111.3	109.5	2.1
363	57.4	61.6	4.2
364	43.2	50.3	7.2
378	74.7	77.0	2.4
379	89.4	87.4	1.9

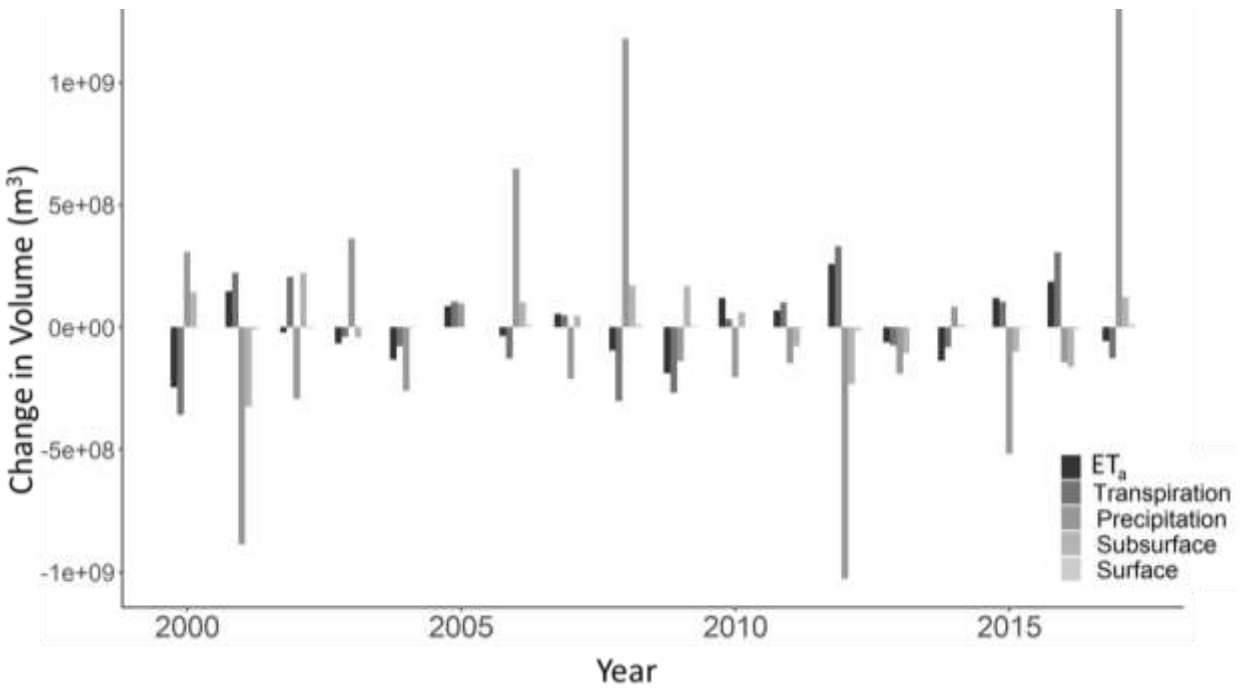
304



305
 306 **Figure 6: Time series outputs from the South Nation watershed HydroGeoSphere (HGS) simulation over the**
 307 **2000-to-2017-time interval. (a) stream flow at the furthest downstream hydrometric station, (b) watershed**
 308 **evapotranspiration, (c) watershed subsurface water storage, and (d) watershed land surface water storage.**

309 The HGS output was generated at variable time steps that were each no larger than 1 day, and then aggregated to
 310 yearly values for use in the ecosystem services assessment (Table 1A). Annual deviations from the long term mean,
 311 for ET_a , transpiration, total precipitation, and surface and subsurface water storage, are presented in Fig. 7. In the

312 context of subsequent analysis and discussion, it should be noted that the drought year of 2012 exhibits the highest
 313 ET_a and transpiration, lowest precipitation, and large drops in both subsurface and surface water storage.



314
 315 **Figure 7: Annual deviation from the long term (2000-2017) mean evapotranspiration, transpiration,**
 316 **precipitation, and subsurface and surface water storages.**

317 **3.2 Valuation of ecosystem services, and average and marginal water productivity**

318 **Table 2: Land use types and unit values for the SNW.**

Land Use	Area (hectare)	Unit value (\$/hectare/year)
Water	1,299	165
Urban	25,734	1,177
Wetlands	16,709	71,273
Grasslands	7,6961	4,152
Croplands	154,810	1,666
Forest	107,470	4,993

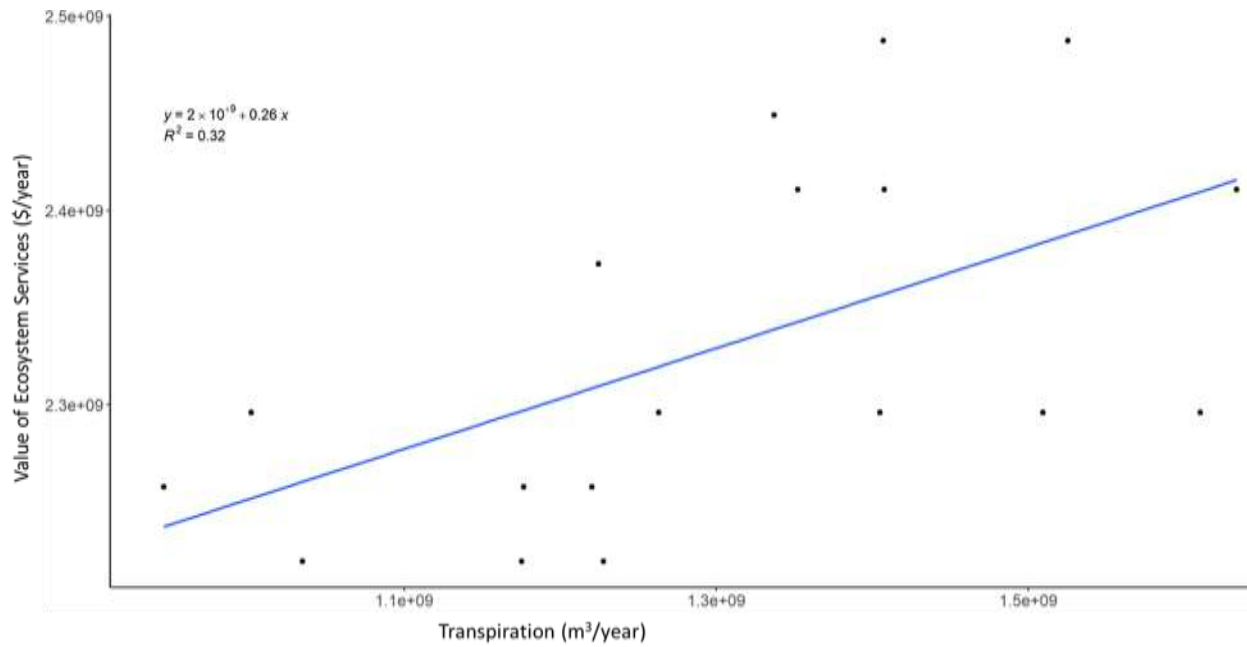
319
 320 Using unit values for the major land use types in the SNW (Table 2) and land use area, total value of the 13 ecosystem
 321 services under consideration is \$2.33 billion per year (in CAD 2022) prior to further annual modifications based on

322 the vegetation indicator (Eq. 1). The estimates for average product of water are point estimates based on the value of
 323 ecosystem services and productive green water volume (i.e., transpiration) for the corresponding year. Annual NPP
 324 data, ES values, transpiration volume, and average water product in the SNW are given in Table 3.

325 **Table 3: Mean Net Primary Production (NPP), ecosystem services (ES) values, transpiration volume, and**
 326 **average product of water for the SNW over the 18-year study interval.**

Year	Mean NPP (Kg C/m ² /year)	ES Value (x10 ⁹ \$/year)	Transpiration (x10 ⁹ m ³)	Average product of water (\$/m ³)
2000	0.59	2.26	0.95	2.39
2001	0.65	2.49	1.53	1.63
2002	0.6	2.30	1.51	1.52
2003	0.6	2.30	1.26	1.82
2004	0.62	2.37	1.22	1.94
2005	0.63	2.41	1.41	1.71
2006	0.58	2.22	1.18	1.89
2007	0.63	2.41	1.35	1.78
2008	0.6	2.30	1.00	2.29
2009	0.58	2.22	1.03	2.14
2010	0.64	2.45	1.34	1.83
2011	0.6	2.30	1.40	1.63
2012	0.63	2.41	1.63	1.48
2013	0.58	2.22	1.23	1.81
2014	0.59	2.26	1.22	1.85
2015	0.65	2.49	1.41	1.77
2016	0.6	2.30	1.61	1.43
2017	0.59	2.26	1.18	1.92

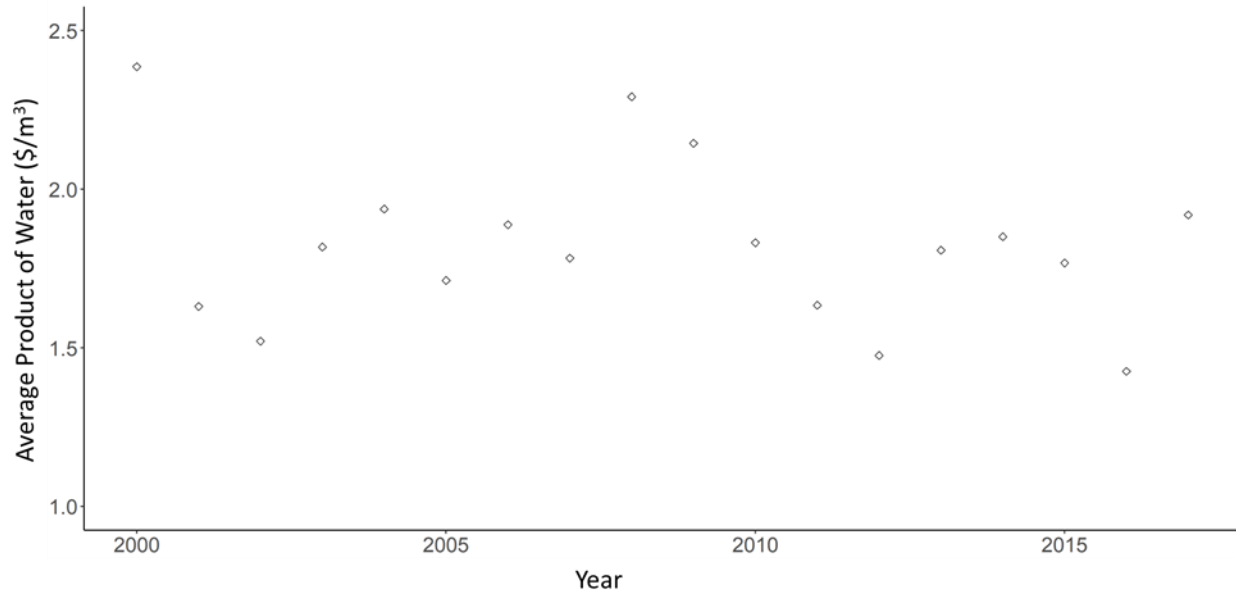
327
 328 For the ecosystem services marginal water productivity, a production function is developed using transpiration and
 329 ES values for the SNW (Fig. 8) and the slope of the function equates to the marginal productivity of water, which is
 330 \$0.26/m³.



331

332 **Figure 8: Ecosystem services water production function for the SNW.**

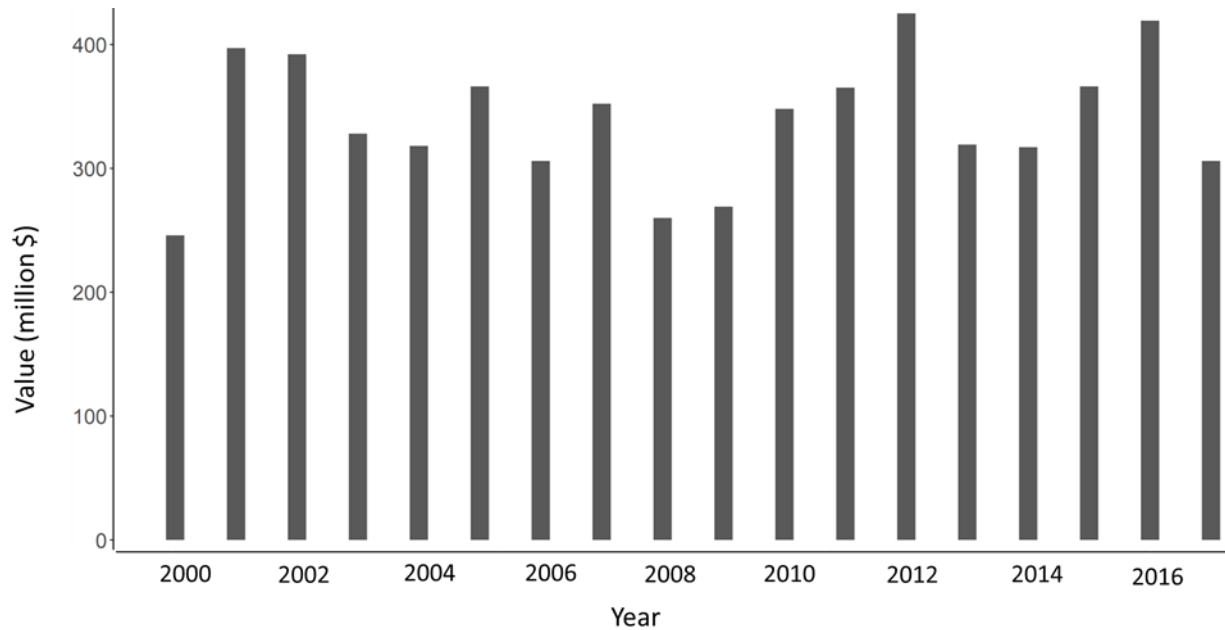
333 To assess the contribution of subsurface water towards ecosystem services, the average ecosystem services water
 334 productivity at the watershed scale is calculated (Table 3). The average product of water over the 18 year study interval
 335 ranges from \$1.43-2.39 per m³ (Fig. 9). During the drought years (2001-2002, 2012 and 2016), the average product
 336 of water declines to local minima. This is because the average product depicts water use efficiency, with the highest
 337 value observed for year 2000 indicating that hydrologic conditions favoured the maximum production of ecosystem
 338 services with the lowest water consumption in that year.



339
 340 **Figure 9: Average annual product of water for ecosystem services in the SNW over the 18-year study period.**

341 **3.3 Valuation of green, subsurface, and surface waters**

342 Using the marginal water productivity and transpiration in the SNW, the value of green water over the study period
 343 was calculated (Fig. 10). The annual values range from \$245.9 (year 2000) to \$424.7 (year 2012) million per year,
 344 with an overall average of \$338.83 million. In general, there is a strong inverse correlation between total annual
 345 precipitation and green water value, with an R^2 of 0.45 ($p < 0.0001$).



346

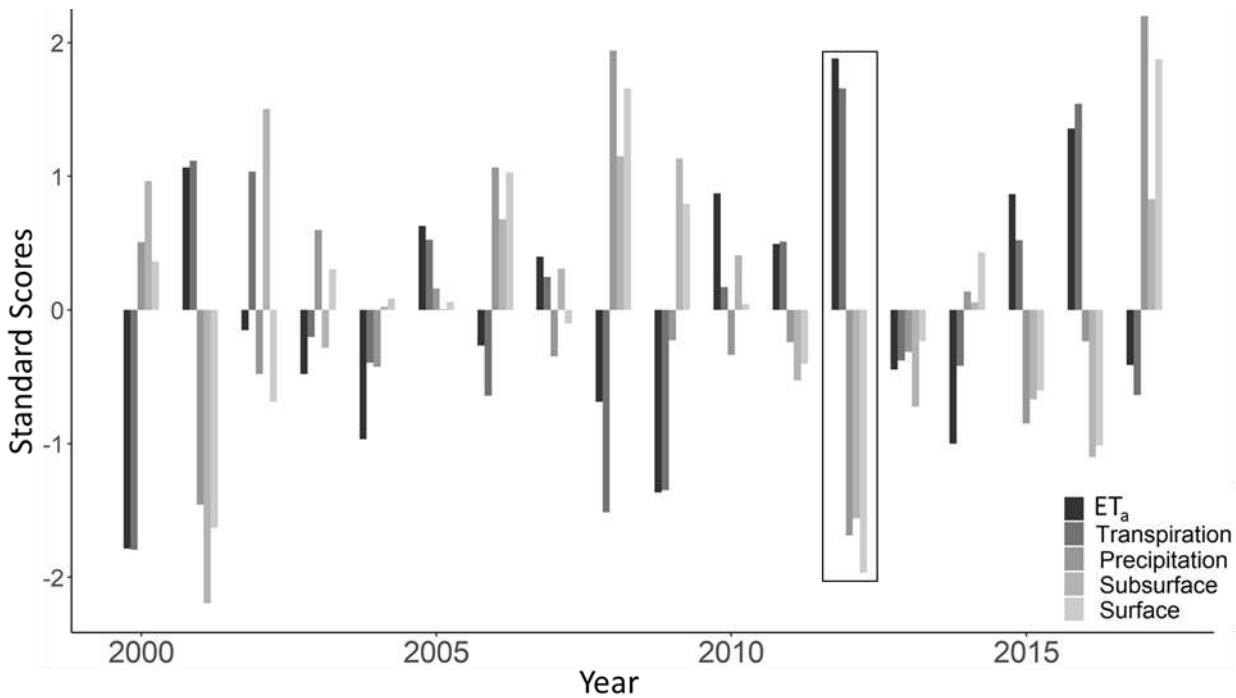
347 **Figure 10: Value of green water in the SNW over the 18-year study period.**

348 **4 Discussion**

349 Transpiration is a key process that sustains terrestrial ecosystem functions such as biomass production, and thus helps
 350 to supply a variety of ecosystem services. In the study herein, HGS is used to capture the contributions of subsurface
 351 water storage to transpiration (i.e., productive green water) and quantify its role in sustaining transpiration and
 352 subsequent ecosystem services.

353 The annual deviations from the long-term means (Fig. 6) show that ET_a and transpiration are supported by the
 354 subsurface and surface storages during droughts. In the drought period from 2001-2002, an interesting situation arises.
 355 In 2001, both ET_a and transpiration exhibit positive values relative to the mean. However, in 2002, despite ET_a being
 356 negative, transpiration remains positive and surpasses the mean value. This deviation can be attributed to the
 357 diminished availability of surface water, leading to reduced evaporation and subsequently lower ET_a . Nevertheless,
 358 transpiration continues to exceed the average due to its reliance on subsurface water availability within the SNW.
 359 Moreover, transpiration primarily relies on biological factors (e.g., land use, NPP), whereas evaporation is
 360 predominantly influenced by meteorological conditions (e.g., air temperature) (Xu et al., 2022). This finding is further
 361 supported by previous studies, which suggest that transpiration dominates ET_a during drought years, while evaporation
 362 takes precedence during wet years (Zhang et al., 2019). To further compare the fluctuations in different storage zones

363 on a common scale, the standard scores (that is, the change in a storage/standard deviation) for each zone are calculated
 364 over time (Fig. 11). The standard scores show that ET_a is supported by both surface and subsurface water storages
 365 during the drought periods. However, the contribution of subsurface water by volume during drought is much larger
 366 than that of surface water, thus highlighting the important role of subsurface water in supporting land surface processes
 367 during droughts.



368
 369 **Figure 11: Change in standard scores of water storages/hydrological variables over the 18-year study period.**
 370 **The scores for the 2012 drought year are bordered.**

371 Comparison of years 2001 and 2012 (both with less precipitation than the 18-year mean) shows that the ET_a was less
 372 but outflow was more in year 2001 than in 2012 (Fig. 6(a)). In such case, it is the subsurface water contribution in
 373 2001 that maintained the higher surface water flows, which highlights the important role of antecedent conditions in
 374 regulating low flow response. The influence of subsurface water on drought behaviour (i.e. years 2001 and 2012) also
 375 depends on the timing of precipitation along with other climatic conditions (e.g., temperature, atmospheric moisture
 376 demand, etc.) in the corresponding years (Zhao et al., 2022). During drought periods, vegetation and atmospheric
 377 moisture demand is often not met, thus resulting in ecosystem stress along with depletion of subsurface and surface
 378 water storages (Zhao et al., 2022). Similar to worldwide trends described in Zhao et al. (2022), the transpiration and
 379 ET_a rates in the SNW increase during dry periods. Given the complexities involved with linking transpiration with

380 subsurface water storages, full characterization of transpiration influences on ecosystem services during droughts has
381 until now received little attention.

382 The study herein is seminal in quantifying subsurface water ecosystem services values, at the scale of a 3830 km²
383 watershed, over a period of time that encompasses wide ranging annual climatology. Previous studies (e.g., Loheide,
384 2008; Su et al., 2022) have estimated groundwater contribution to evapotranspiration by linking water table
385 fluctuation with changes in evapotranspiration. However, over large areas, using water table fluctuation can be
386 complicated by other subsurface water sinks, including deeper groundwater recharge and discharge into surface water
387 receptors. With the HGS approach employed herein, the computed subsurface water evaporation and transpiration,
388 and surface water evaporation, in conjunction with the other hydrologic flow processes depicted in Fig. 2, provides a
389 robust characterization of contributions to ET_a.

390 The fluctuations in water storages show that, in general and with respect to longer term mean conditions, subsurface
391 water storage repletes when ET_a is negative and depletes when ET_a is positive. In both the 2001 and 2012 drought
392 years, ET_a is relatively high in comparison to the wet years with high precipitation. ET_a in drought years is primarily
393 supported by the drawdown (by volume) in subsurface water storage below the mean level. In general, fluctuations in
394 subsurface water storage across the 18 years are consistent with changes in precipitation, with above-average
395 precipitation aligned with increases in subsurface water storage and vice-versa. In contrast, increased ET_a leads to a
396 reduction in subsurface storage and vice-versa. Over the 18 year study period, the maximum increase in subsurface
397 water storage occurred in the year 2002, immediately following the 2001 drought which had implications far beyond
398 just the SNW (Wheaton et al., 2008). Even though 2002 was a year with less than average precipitation, the drought
399 impacted subsurface storage conditions led to an antecedent condition across the SNW that was conducive to
400 subsurface water recharge.

401 Regarding the economic valuation of water components, green water mainly benefits people at local scales (by
402 supporting biomass and ecosystem services in the area) whereas the benefits of blue water are seen at larger scales
403 (Falkenmark and Rockström, 2010). Incorporating green-blue water resource consideration at the watershed scale
404 helps with the characterization and quantification of the role water plays in land use and terrestrial ecosystem function.
405 Based on the study herein, fully-integrated groundwater – surface water models, such as HGS, have potential to
406 facilitate better management of watershed scale (approximately 4,000 km²) water resources for ecosystem services
407 endpoints, and to evaluate the contributions of terrestrial water storages towards green water supply.

408 A water production function was developed using total green water volumes and total values of 13 ecosystem services
409 in the SNW: agricultural services (net benefits from the crops or agricultural products), global climate regulation, air
410 quality, water provision, waste treatment, erosion control, pollination, habitat for biodiversity, natural hazard
411 prevention, pest management, nutrient cycling, landscape aesthetics, and recreational activities. The ecosystem water
412 production function yields a marginal value of \$ 0.26 per m³ of green water (or transpiration) (Fig. 8). Globally, Lowe
413 et al. (2022) estimated the average marginal product of water specifically for crop production at \$0.083 per m³.
414 Additional transpiration supplies ecosystem services at a constant rate; however, because the linear line of best fit in
415 Fig. 8 has a positive vertical intercept, the average ecosystem services water productivity decreases with increase in
416 transpiration as the slope of the ray from origin through a point on production function diminishes (Wichelns, 2014).
417 Hence, while water productivity is greatest when the smallest amount of water is used/consumed, it also produces the
418 smallest value of ecosystem services at this point. Between 2000 and 2017, transpiration in the SNW is highest during
419 the driest years in response to drought-associated meteorological conditions such as increase in temperatures (Zhao et
420 al., 2022). However, NPP does not decline during the drought periods, which is consistent with other temperate
421 watershed studies (e.g., Hosen et al., 2019; Sun et al., 2016). Modeling results presented herein show that the drought-
422 induced water stress increases both transpiration and ET_a rates, similar to Zhao et al. (2022) and Diao et al. (2021).
423 During dry years, the increase in transpiration is positively correlated with higher NPP, which in turn relates to lower
424 ecosystem services water productivity (Fig. 9).

425 In the SNW, green water use increases in dry years with less than average precipitation. Accordingly, green water
426 value was highest, at \$424.7 million (in CAD 2022), for the 2012 drought year (Fig. 10). It is important to note that
427 value of the subsurface water contribution is second highest, at 418.63 million, for 2016, which is also a drought year.
428 Hence, the critical role of subsurface water in sustaining ecosystem services is evident during both drought years and
429 more typical years.

430 While the study herein advances the scientific utility of physics-based fully-integrated groundwater–surface water
431 models, it is essential to acknowledge the inherent uncertainty associated with such an analysis, along with factors
432 that could potentially reduce this uncertainty. It is well known that highly parameterized, structurally complex models
433 can have many degrees of freedom, high data requirements, and non-uniqueness challenges (Beven, 2006). However,
434 the parameterization of physics-based models can also be viewed as a strength due to the constraining relationship
435 between physically measurable characteristics and parameter values (Ebel and Loague, 2006). For the SNW, soil and

436 subsurface materials are well characterized and hence the spatial distribution and magnitudes of the associated
437 hydraulic parameters are generally well represented in the HGS model. Incorporating meteorological variability into
438 structurally complex model calibration and performance evaluation can also act to reduce uncertainty (Moeck et al.,
439 2018). Because the SNW simulation extended over an 18-year time frame that included multiple droughts and floods,
440 there is confidence that the model structure and parameterization is suited for a wide spectrum of hydrologic
441 conditions, and that the model can dynamically capture transitions from wet-to-dry and dry-to-wet conditions, which
442 is a critical part of the SNW analysis.

443 It can be posited that physics-based models are best suited for the type of challenge addressed in the work herein
444 because simpler models lack process representation critical within the problem conceptualization (Ebel and Loague,
445 2006). This can be deemed especially true when considering difficulties associated with quantifying large scale
446 evaporation and transpiration (Stoy et al., 2019), and groundwater–surface water interaction (Barthel and Banzhaf,
447 2016). Structurally complex models have been shown to perform better than simple models when simulating
448 evapotranspiration (Ghasemizade et al., 2015) and groundwater recharge (Moeck et al., 2018), and previous work by
449 Hwang et al. (2015) demonstrated the utility of HGS for constraining ET at the watershed scale within the same
450 geographic region as the SNW. Further confidence in the SNW HGS model can be established through comparison
451 with other studies. In terms of overall water balance, results from the study herein compare closely with data compiled
452 as part of regional water management study encompassing the SNW (EOWRMS, 2001). Although the study time
453 frames differ (the EOWRMS (2001) study utilized pre-2000 data), the results are similar, with ETa accounting for
454 approximately 45 % and 62 % of annual precipitation in EOWRMS (2001) and the study herein, respectively. While
455 there is limited previous work investigating the partitioning of ETa into transpiration and evaporation that can be
456 directly compared, it is useful to refer to highly detailed analysis based off Fluxnet data (Pastorello et al., 2020) as
457 reference for transpiration and evaporation partitioning in landcover settings representative of those within the SNW.
458 For example, Xue et al. (2023) reported that transpiration as a percentage of ET ranged from 21-56 % and 39-83 % in
459 Fluxnet cropland and mixed forest settings, respectively, whereas the HGS model predicts an aggregate range of 45-
460 65 % across the SNW watershed, which supports the use of HGS transpiration estimates in subsequent ecosystem
461 services valuation.

462 The methodology employed in this study provides a basis for deploying fully-integrated groundwater – surface water
463 models to assess subsurface water contribution to ecosystem services in other regions. However, it must be noted that

464 the results and values used herein are not necessarily transferable to other sites/watersheds. The marginal product of
465 water is a site-specific entity that will be different for other watersheds because both ecosystem services value and
466 transpiration rate will change in response to factors such as land cover, NPP, climate/weather, hydrogeology, and soil
467 properties. Nevertheless, given the ability of fully-integrated models to quantify the dynamic fluctuation in water
468 storages across different compartments, along with the linkage to terrestrial ecosystem services, the approach can be
469 expected to yield reliable results under similar workflow (modelling of water storages and transpiration rates, and
470 valuation of ecosystem services) for other locations/sites/watersheds.

471 **5 Conclusions**

472 This study characterizes and quantifies the important contribution of subsurface water towards the supply of terrestrial
473 ecosystem services, which, until now has not been comprehensively studied. The prior lack of attention to subsurface
474 water in part relates to the complexities involved with characterizing the dynamic movement of water between
475 subsurface water and surface water storage compartments, and the related supply of green water. In the work herein,
476 focusing on a 3830 km² mixed use watershed, the innovative use of a HGS fully-integrated groundwater – surface
477 water model for water ecosystem services valuation is demonstrated, with the endpoint being monetization of the
478 contributions of subsurface water to green water supply over a period of 18 years (2000-2017). Results show that
479 droughts are a major impetus for increased green water use. The maximum annual green water value was \$424.7
480 million (CAD 2022) during the 2012 drought year, while the 18-year average was \$338.83 million. Similarly, in other
481 dry years (i.e., 2001-2002 and 2016), there was a discernible rise in the green water use. Conversely, the results show
482 a notable decrease in the green water use during years characterized by higher precipitation, as exemplified in the year
483 2000 where green water provided \$245.9 million in ecosystem services value. Hence, the study emphasizes the key
484 role of subsurface water in supplying green water and sustaining ecosystem services during critical periods when the
485 watershed is under meteorological drought. The methodology developed herein is extensible to other watersheds and
486 provides the ability to improve characterization of water ecosystem services and to better value and manage subsurface
487 water resources under current and future climate conditions.

488 **Author contribution**

489 Tariq Aziz contributed to concept development, methodology, formal analysis, investigation, and writing the original
490 draft.

491 Steven K. Frey contributed to concept development, methodology, data curation, HGS modeling, project
492 administration, and reviewing and editing the manuscript.

493 David R. Lapen contributed to methodology development, reviewing and editing the manuscript, and project
494 administration.

495 Susan Preston contributed to methodology development, reviewing and editing the manuscript, and project
496 administration.

497 Hazen A. J. Russell contributed to hydrogeologic characterization, and with reviewing and editing the manuscript.

498 Omar Khader contributed to data curation, HGS model development, and formal analysis.

499 Andre R. Erler contributed to data curation and reviewing the manuscript.

500 Edward A. Sudicky contributed to project administration and reviewing the manuscript.

501 **Declaration of interest**

502 The authors declare that they have no known competing financial interests or personal relationships that could have
503 appeared to influence the work reported in this paper.

504 **References**

505 Agriculture and Agri-Food Canada: Annual Space-Based Crop Inventory for Canada, 2017, Agroclimate, Geomatics
506 and Earth Observation Division, Science and Technology Branch, 2017.

507 Allen, R. G., Pereira, L. S., Raes, D., and Smith, M.: Crop evapotranspiration guidelines for computing crop
508 requirements, 1998. Available at: <https://www.fao.org/3/X0490E/x0490e00.htm>

509 An, S. and Verhoeven, J. T. A.: Wetlands: Ecosystem services, restoration and wise use, Springer, 325 pp.,
510 <https://doi.org/10.1007/978-3-030-14861-4>, 2019.

511 Aquanty: HydroGeoSphere: A three-dimensional numerical model describing fully-integrated subsurface and surface
512 flow and solute transport, Waterloo, 2021.

513 Arnold, J. G., Srinivasan, R., Muttiah, R. S., and Williams, J. R.: Large area hydrologic modeling and assessment part
514 I: Model development, *J. Am. Water Resour. Assoc.*, 34, 73–89, <https://doi.org/10.1111/j.1752-1688.1998.tb05961.x>,
515 1998.

516 Aziz, T.: Changes in land use and ecosystem services values in Pakistan, 1950–2050, *Environ. Dev.*, 35, 13,
517 <https://doi.org/10.1016/j.envdev.2020.100576>, 2021.

518 Barthel, R. and Banzhaf, S.: Groundwater and Surface Water Interaction at the Regional-scale – A Review with Focus
519 on Regional Integrated Models, *Water Resour. Manag.*, 30, 1–32, <https://doi.org/10.1007/s11269-015-1163-z>, 2016.

520 Berg, S. J. and Sudicky, E. A.: Toward Large-Scale Integrated Surface and Subsurface Modeling, *Groundwater*, 57,
521 1–2, <https://doi.org/10.1111/gwat.12844>, 2019.

522 Beven, K.: A manifesto for the equifinality thesis, *J. Hydrol.*, 320, 18–36,
523 <https://doi.org/10.1016/j.jhydrol.2005.07.007>, 2006.

524 Bolte, J.: *Envision integrated modeling platform*, 94 pp., 2022.

525 Booth, E. G., Zipper, S. C., Loheide, S. P., and Kucharik, C. J.: Is groundwater recharge always serving us well?
526 Water supply provisioning, crop production, and flood attenuation in conflict in Wisconsin, USA, *Ecosyst. Serv.*, 21,
527 153–165, 2016.

528 Brunner, P. and Simmons, C. T.: *HydroGeoSphere: A Fully Integrated, Physically Based Hydrological Model*, *Ground*
529 *Water*, 50, 170–176, <https://doi.org/10.1111/j.1745-6584.2011.00882.x>, 2012.

530 Casagrande, E., Recanatì, F., Cristina, M., Bevacqua, D., and Meli, P.: Water balance partitioning for ecosystem
531 service assessment. A case study in the Amazon, *Ecol. Indic.*, 121, <https://doi.org/10.1016/j.ecolind.2020.107155>,
532 2021.

533 Chen, X. and Hu, Q.: Groundwater influences on soil moisture and surface evaporation, *J. Hydrol.*, 297, 285–300,
534 <https://doi.org/10.1016/j.jhydrol.2004.04.019>, 2004.

535 Clark, M. P., Fan, Y., Lawrence, D. M., Adam, J. C., Bolster, D., Gochis, D. J., Hooper, R. P., Kumar, M., Leung, L.
536 R., Mackay, D. S., and Maxwell, R. M.: Hydrological partitioning in the critical zone: Recent advances and
537 opportunities for developing transferable understanding of water cycle dynamics, *Water Resour. Res.*, 1–28,
538 <https://doi.org/10.1002/2015WR017096>.Received, 2015.

539 Condon, L. E., Atchley, A. L., and Maxwell, R. M.: Evapotranspiration depletes groundwater under warming over the
540 contiguous United States, *Nat. Commun.*, 11, <https://doi.org/10.1038/s41467-020-14688-0>, 2020.

541 Costanza, R., D’Arge, R., De Groot, R., Farber, S., Grasso, M., Hannon, B., Limburg, K., Naeem, S., O’Neill, R. V.,
542 Paruelo, J., Raskin, R. G., Sutton, P., and Van Den Belt, M.: The value of ecosystem services: Putting the issues in
543 perspective, *Ecol. Econ.*, 25, 67–72, [https://doi.org/10.1016/S0921-8009\(98\)00019-6](https://doi.org/10.1016/S0921-8009(98)00019-6), 1998.

544 Decsi, B., Ács, T., Jolánkai, Z., Kardos, M. K., Kóncsos, L., Vári, Á., and Kozma, Z.: From simple to complex –
545 Comparing four modelling tools for quantifying hydrologic ecosystem services, *Ecol. Indic.*, 141,
546 <https://doi.org/10.1016/j.ecolind.2022.109143>, 2022.

547 Dennedy-Frank, P. J., Muenich, R. L., Chaubey, I., and Ziv, G.: Comparing two tools for ecosystem service
548 assessments regarding water resources decisions, *J. Environ. Manage.*, 177, 331–340,
549 <https://doi.org/10.1016/j.jenvman.2016.03.012>, 2016.

550 Diao, H., Wang, A., Yang, H., Yuan, F., Guan, D., and Wu, J.: Responses of evapotranspiration to droughts across
551 global forests: A systematic assessment, *Can. J. For. Res.*, 51, 1–9, <https://doi.org/10.1139/cjfr-2019-0436>, 2021.

552 Ebel, B. A. and Loague, K.: Physics-based hydrologic-response simulation: Seeing through the fog of equifinality,
553 *Hydrol. Process.*, 20, 2887–2900, <https://doi.org/10.1002/hyp.6388>, 2006.

554 Endsley, K. A., Zhao, M., Kimball, J., and Deva, S.: Continuity of global MODIS terrestrial primary productivity
555 estimates in the VIIRS era using model-data fusion, *J. Geophys. Res. Biogeosciences*,
556 <https://doi.org/10.22541/essoar.167768101.16068273/v1>, 2023.

557 EOWRMS: *Eastern Ontario water resources management study (final report)*, Ottawa, Ontario, 5–24 pp., 2001.

558 Erler, A. R., Frey, S. K., Khader, O., d’Orgeville, M., Park, Y. J., Hwang, H. T., Lapen, D. R., Richard Peltier, W.,

559 and Sudicky, E. A.: Simulating Climate Change Impacts on Surface Water Resources Within a Lake-Affected Region
560 Using Regional Climate Projections, *Water Resour. Res.*, 55, 130–155, <https://doi.org/10.1029/2018WR024381>,
561 2019.

562 Falkenmark, M. and Rockström, J.: Building Water Resilience in the Face of Global Change: From a Blue-Only to a
563 Green-Blue Water Approach to Land-Water Management, *J. Water Resour. Plan. Manag.*, 136, 606–610,
564 [https://doi.org/10.1061/\(asce\)wr.1943-5452.0000118](https://doi.org/10.1061/(asce)wr.1943-5452.0000118), 2010.

565 Foster, S. S. D. and Chilton, P. J.: Groundwater: The processes and global significance of aquifer degradation, *Philos.*
566 *Trans. R. Soc. B Biol. Sci.*, 358, 1957–1972, <https://doi.org/10.1098/rstb.2003.1380>, 2003.

567 Frey, S. K., Miller, K., Khader, O., Taylor, A., Morrison, D., Xu, X., Berg, S. J., Sudicky, E. A., and Lapen, D. R.:
568 Evaluating landscape influences on hydrologic behavior with a fully- integrated groundwater – surface water model,
569 *J. Hydrol.*, 602, 1–8, 2021.

570 Ghasemizade, M., Moeck, C., and Schirmer, M.: The effect of model complexity in simulating unsaturated zone flow
571 processes on recharge estimation at varying time scales, *J. Hydrol.*, 529, 1173–1184,
572 <https://doi.org/10.1016/j.jhydrol.2015.09.027>, 2015.

573 Griebler, C. and Avramov, M.: Groundwater ecosystem services: A review, *Freshw. Sci.*, 34, 355–367,
574 <https://doi.org/10.1086/679903>, 2015.

575 Hogg, E. H.: Temporal scaling of moisture and the forest-grassland boundary in western Canada, *Agric. For.*
576 *Meteorol.*, 84, 115–122, [https://doi.org/10.1016/S0168-1923\(96\)02380-5](https://doi.org/10.1016/S0168-1923(96)02380-5), 1997.

577 Honeck, E., Gallagher, L., von Arx, B., Lehmann, A., Wyler, N., Villarrubia, O., Guinaudeau, B., and Schlaepfer, M.
578 A.: Integrating ecosystem services into policymaking – A case study on the use of boundary organizations, *Ecosyst.*
579 *Serv.*, 49, <https://doi.org/10.1016/j.ecoser.2021.101286>, 2021.

580 Hosen, J. D., Aho, K. S., Appling, A. P., Creech, E. C., Fair, J. H., Hall, R. O., Kyzivat, E. D., Lowenthal, R. S., Matt,
581 S., Morrison, J., Sainers, J. E., Shanley, J. B., Weber, L. C., Yoon, B., and Raymond, P. A.: Enhancement of primary
582 production during drought in a temperate watershed is greater in larger rivers than headwater streams, *Limnol.*
583 *Oceanogr.*, 64, 1458–1472, <https://doi.org/10.1002/lno.11127>, 2019.

584 Hwang, H. T., Park, Y. J., Frey, S. K., Berg, S. J., and Sudicky, E. A.: A simple iterative method for estimating
585 evapotranspiration with integrated surface/subsurface flow models, *J. Hydrol.*, 531, 949–959,
586 <https://doi.org/10.1016/j.jhydrol.2015.10.003>, 2015.

587 Jin, Z., Liang, W., Yang, Y., Zhang, W., Yan, J., Chen, X., Li, S., and Mo, X.: Separating Vegetation Greening and
588 Climate Change Controls on Evapotranspiration trend over the Loess Plateau, *Sci. Rep.*, 7, 1–15,
589 <https://doi.org/10.1038/s41598-017-08477-x>, 2017.

590 Kollet, S., Mauro, S., M., M. R., Paniconi, C., Putti, M., Bertoldi, G., Coon, E. T., Cordano, E., Endrizzi, S., Kikinzon,
591 E., Mouche, E., M€ugler, C., Park, Y.-J., Refsgaard, J. C., Stisen, S., and Sudicky, E.: The integrated hydrologic model
592 intercomparison project, IH-MIP2: A second set of benchmark results to diagnose integrated hydrology and feedbacks,
593 *Water Resour. Res.*, 867–890, <https://doi.org/10.1002/2016WR019191>.Received, 2016.

594 Kornelsen, K. C. and Coulibaly, P.: Synthesis review on groundwater discharge to surface water in the Great Lakes
595 Basin, *J. Great Lakes Res.*, 40, 247–256, <https://doi.org/10.1016/j.jglr.2014.03.006>, 2014.

596 L'Ecuyer-Sauvageau, C., Dupras, J., He, J., Auclair, J., Kermagoret, C., and Poder, T. G.: The economic value of
597 Canada's National Capital Green Network, *PLoS One*, 16, 1–29, <https://doi.org/10.1371/journal.pone.0245045>, 2021.

598 Li, Q., Qi, J., Xing, Z., Li, S., Jiang, Y., Danieleescu, S., Zhu, H., Wei, X., and Meng, F. R.: An approach for assessing
599 impact of land use and biophysical conditions across landscape on recharge rate and nitrogen loading of groundwater,
600 *Agric. Ecosyst. Environ.*, 196, 114–124, <https://doi.org/10.1016/j.agee.2014.06.028>, 2014.

601 Liang, X., Lettenmaier, D. P., Wood, E. F., and Burges, S. J.: A simple hydrologically based model of land surface
602 water and energy fluxes for general circulation models, *J. Geophys. Res.*, 99, <https://doi.org/10.1029/94jd00483>, 1994.

603 Liu, Y. and El-Kassaby, Y. A.: Evapotranspiration and favorable growing degree-days are key to tree height growth
604 and ecosystem functioning: Meta-Analyses of Pacific Northwest historical data, 1st Annu. IEEE Conf. Control
605 Technol. Appl. CCTA 2017, 2017-Janua, 7–12, <https://doi.org/10.1038/s41598-018-26681-1>, 2017.

606 Liu, Y., Zhou, R., Wen, Z., Khalifa, M., Zheng, C., Ren, H., Zhang, Z., and Wang, Z.: Assessing the impacts of
607 drought on net primary productivity of global land biomes in different climate zones, *Ecol. Indic.*, 130, 108146,
608 <https://doi.org/10.1016/j.ecolind.2021.108146>, 2021.

609 Logan, C., Cummings, D. I., Pullan, S., Pugin, A., Russell, H. A. J., and Sharpe, D. R.: Hydrostratigraphic model of
610 the South Nation watershed region, south-eastern Ontario, Geological Survey of Canada, 17 pp.,
611 <https://doi.org/https://doi.org/10.4095/248203>, 2009.

612 Loheide, S. P.: A method for estimating subdaily evapotranspiration of shallow groundwater using diurnal water table
613 fluctuations, *Ecohydrology*, 1, 59–66, 2008.

614 Lowe, B. H., Zimmer, Y., and Oglethorpe, D. R.: Estimating the economic value of green water as an approach to
615 foster the virtual green-water trade, *Ecol. Indic.*, 136, 108632, <https://doi.org/10.1016/j.ecolind.2022.108632>, 2022.

616 Mammola, S., Cardoso, P., Culver, D. C., Deharveng, L., Ferreira, R. L., Fišer, C., Galassi, D. M. P., Griebler, C.,
617 Halse, S., Humphreys, W. F., Isaia, M., Malard, F., Martinez, A., Moldovan, O. T., Niemiller, M. L., Pavlek, M.,
618 Reboleira, A. S. P. S., Souza-Silva, M., Teeling, E. C., Wynne, J. J., and Zagnajster, M.: Scientists' warning on the
619 conservation of subterranean ecosystems, *Bioscience*, 69, 641–650, <https://doi.org/10.1093/biosci/biz064>, 2019.

620 Maxwell, R. M., Putti, M., Meyerhoff, S., Delfs, J.-O., Ferguson, I. M., Ivanov, V., Jongho Kim, O. K., Stefan J.
621 Kollet, M. K., Lopez, S., Jie Niu, Claudio Paniconi, Y.-J. P., Mantha S. Phanikumar, C. S., Sudicky, E. A., and Sulis,
622 M.: Surface-subsurface model intercomparison: A first set of benchmark results to diagnose integrated hydrology and
623 feedbacks, *Water Resour. Res.*, 1531–1549, <https://doi.org/10.1002/2013WR013725>.Received, 2014.

624 McKenney, D. W., Hutchinsson, M. F., Papadopol, P., Lawrence, K., Pedlar, J., Campbell, K., Milewska, E.,
625 Hopkinson, R. F., Price, D., and Owen, T.: Customized spatial climate models for North America, *Bull. Am. Meteorol.*
626 *Soc.*, 92, 1611–1622, <https://doi.org/10.1175/2011BAMS3132.1>, 2011.

627 Mercado-bettín, D., Salazar, J. F., and Villegas, J. C.: Long-term water balance partitioning explained by physical and
628 ecological characteristics in world river basins, *Ecohydrology*, 12, 1–13,
629 <https://doi.org/https://doi.org/10.1002/eco.2072>, 2019.

630 Millenium Ecosystem Assessment (MEA): Ecosystems and Human Well-Being: Synthesis, Island Press, 285 pp.,
631 <https://doi.org/10.1057/9780230625600>, 2005.

632 Moeck, C., von Freyberg, J., and Schirmer, M.: Groundwater recharge predictions in contrasted climate: The effect of

633 model complexity and calibration period on recharge rates, *Environ. Model. Softw.*, 103, 74–89,
634 <https://doi.org/10.1016/j.envsoft.2018.02.005>, 2018.

635 Moriasi, D. N., Arnold, J. G., Van Liew, M. W., Bingner, R. L., Harmel, R. D., and Veith, T. L.: Model evaluation
636 guidelines for systematic quantification of accuracy in watershed simulations, *Trans. ASABE*, 50, 885–900,
637 <https://doi.org/10.13031/2013.23153>, 2007.

638 Mulligan, M.: User guide for the Co\$ting Nature Policy Support System v.2., <https://goo.gl/Grpbnb>, 2015.

639 Muñoz-Sabater, J., Dutra, E., Agustí-Panareda, A., Albergel, C., Arduini, G., Balsamo, G., Boussetta, S., Choulga,
640 M., Harrigan, S., Hersbach, H., Martens, B., Miralles, D. G., Piles, M., Rodríguez-Fernández, N. J., Zsoter, E.,
641 Buontempo, C., and Thépaut, J. N.: ERA5-Land: A state-of-the-art global reanalysis dataset for land applications,
642 *Earth Syst. Sci. Data*, 13, 4349–4383, <https://doi.org/10.5194/essd-13-4349-2021>, 2021.

643 MYD15A2H MODIS/Aqua Leaf Area Index/FPAR 8-Day L4 Global 500m SIN Grid. NASA LP DAAC:
644 Natural Capital Project: InVEST User Guide 3.12.0, 1–7 pp., 2022.

645 Neff, B. P., Day, S. M., Piggott, A. R., and Fuller, L. M.: Base flow in the Great Lakes basin, *U.S. Geol. Surv. Sci.*
646 *Investig. Rep.*, 32, 2005.

647 Ochoa, V. and Urbina-Cardona, N.: Tools for spatially modeling ecosystem services: Publication trends, conceptual
648 reflections and future challenges, *Ecosyst. Serv.*, 26, 155–169, <https://doi.org/10.1016/j.ecoser.2017.06.011>, 2017.

649 Ontario Geological Survey: Surficial Geology of Southern Ontario, Miscellaneous Release--Data 128-REV. Ontario
650 Geological Survey., 1–7 pp., 2010.

651 Ontario Integrated Hydrology Data: [https://geohub.lio.gov.on.ca/maps/mnrf::ontario-integrated-hydrology-oih-](https://geohub.lio.gov.on.ca/maps/mnrf::ontario-integrated-hydrology-oih-data/about)
652 [data/about](https://geohub.lio.gov.on.ca/maps/mnrf::ontario-integrated-hydrology-oih-data/about).

653 Pastorello, G., Trotta, C., Canfora, E., Chu, H., Christianson, D., Cheah, Y. W., Poindexter, C., Chen, J., Elbashandy,
654 A., Humphrey, M., Isaac, P., Polidori, D., Ribeca, A., van Ingen, C., Zhang, L., Amiro, B., Ammann, C., Arain, M.
655 A., Ardö, J., Arkebauer, T., Arndt, S. K., Arriga, N., Aubinet, M., Aurela, M., Baldocchi, D., Barr, A., Beamesderfer,
656 E., Marchesini, L. B., Bergeron, O., Beringer, J., Bernhofer, C., Berveiller, D., Billesbach, D., Black, T. A., Blanken,
657 P. D., Bohrer, G., Boike, J., Bolstad, P. V., Bonal, D., Bonnefond, J. M., Bowling, D. R., Bracho, R., Brodeur, J.,
658 Brümmer, C., Buchmann, N., Burban, B., Burns, S. P., Buysse, P., Cale, P., Cavagna, M., Cellier, P., Chen, S., Chini,
659 I., Christensen, T. R., Cleverly, J., Collalti, A., Consalvo, C., Cook, B. D., Cook, D., Coursolle, C., Cremonese, E.,
660 Curtis, P. S., D’Andrea, E., da Rocha, H., Dai, X., Davis, K. J., De Cinti, B., de Grandcourt, A., De Ligne, A., De
661 Oliveira, R. C., Delpierre, N., Desai, A. R., Di Bella, C. M., di Tommasi, P., Dolman, H., Domingo, F., Dong, G.,
662 Dore, S., Duce, P., Dufrêne, E., Dunn, A., Dušek, J., Eamus, D., Eichelmann, U., ElKhidir, H. A. M., Eugster, W.,
663 Ewenz, C. M., Ewers, B., Famulari, D., Fares, S., Feigenwinter, I., Feitz, A., Fensholt, R., Filippa, G., Fischer, M.,
664 Frank, J., Galvagno, M., Gharun, M., Gianelle, D., et al.: The FLUXNET2015 dataset and the ONEFlux processing
665 pipeline for eddy covariance data, *Sci. Data*, 7, 1–27, <https://doi.org/10.1038/s41597-020-0534-3>, 2020.

666 Qiu, J., Zipper, S. C., Motew, M., Booth, E. G., Kucharik, C. J., and Loheide, S. P.: Nonlinear groundwater influence
667 on biophysical indicators of ecosystem services, *Nat. Sustain.*, 2, 475–483, [https://doi.org/10.1038/s41893-019-0278-](https://doi.org/10.1038/s41893-019-0278-2)
668 [2](https://doi.org/10.1038/s41893-019-0278-2), 2019.

669 Richardson, M. and Kumar, P.: Critical Zone services as environmental assessment criteria in intensively managed

670 landscapes, *Earth's Futur.*, 5, 617–632, <https://doi.org/10.1002/2016EF000517>, 2017.

671 Schaap, M. G., Leij, F. J., and Van Genuchten, M. T.: Rosetta: A computer program for estimating soil hydraulic
672 parameters with hierarchical pedotransfer functions, *J. Hydrol.*, 251, 163–176, <https://doi.org/10.1016/S0022->
673 1694(01)00466-8, 2001.

674 Schyns, J. F., Hoekstra, A. Y., Booij, M. J., Hogeboom, R. J., and Mekonnen, M. M.: Limits to the world's green
675 water resources for food, feed, fiber, timber, and bioenergy, *Proc. Natl. Acad. Sci. U. S. A.*, 116, 4893–4898,
676 <https://doi.org/10.1073/pnas.1817380116>, 2019.

677 Siebert, S., Burke, J., Faures, J. M., Frenken, K., Hoogeveen, J., Döll, P., and Portmann, F. T.: Groundwater use for
678 irrigation - A global inventory, *Hydrol. Earth Syst. Sci.*, 14, 1863–1880, <https://doi.org/10.5194/hess-14-1863-2010>,
679 2010.

680 SLC: Soil Landscapes of Canada Version 3.2, 2007–2008 pp., 2010.

681 Stoy, P. C., El-Madany, T. S., Fisher, J. B., Gentine, P., Gerken, T., Good, S. P., Klosterhalfen, A., Liu, S., Miralles,
682 D. G., Perez-Priego, O., Rigden, A. J., Skaggs, T. H., Wohlfahrt, G., Anderson, R. G., Coenders-Gerrits, A. M. J.,
683 Jung, M., Maes, W. H., Mammarella, I., Mauder, M., Migliavacca, M., Nelson, J. A., Poyatos, R., Reichstein, M.,
684 Scott, R. L., and Wolf, S.: Reviews and syntheses: Turning the challenges of partitioning ecosystem evaporation and
685 transpiration into opportunities, *Biogeosciences*, 16, 3747–3775, <https://doi.org/10.5194/bg-16-3747-2019>, 2019.

686 Su, Y., Feng, Q., Zhu, G., Wang, Y., and Zhang, Q.: A New Method of Estimating Groundwater Evapotranspiration
687 at Sub-Daily Scale Using Water Table Fluctuations, *Water (Switzerland)*, 14, 1–14,
688 <https://doi.org/10.3390/w14060876>, 2022.

689 Sun, B., Zhao, H., and Wang, X.: Effects of drought on net primary productivity: Roles of temperature, drought
690 intensity, and duration, *Chinese Geogr. Sci.*, 26, 270–282, <https://doi.org/10.1007/s11769-016-0804-3>, 2016.

691 Sun, G., Hallema, D., and Asbjornsen, H.: Ecohydrological processes and ecosystem services in the Anthropocene: a
692 review, *Ecol. Process.*, 6, <https://doi.org/10.1186/s13717-017-0104-6>, 2017.

693 Tan, S., Wang, H., Prentice, I. C., and Yang, K.: Land-surface evapotranspiration derived from a first-principles
694 primary production model, *Environ. Res. Lett.*, 16, <https://doi.org/10.1088/1748-9326/ac29eb>, 2021.

695 Taylor, R. G., Scanlon, B., Döll, P., Rodell, M., Van Beek, R., Wada, Y., Longuevergne, L., Leblanc, M., Famiglietti,
696 J. S., Edmunds, M., Konikow, L., Green, T. R., Chen, J., Taniguchi, M., Bierkens, M. F. P., Macdonald, A., Fan, Y.,
697 Maxwell, R. M., Yechieli, Y., Gurdak, J. J., Allen, D. M., Shamsudduha, M., Hiscock, K., Yeh, P. J. F., Holman, I.,
698 and Treidel, H.: Ground water and climate change, *Nat. Clim. Chang.*, 3, 322–329,
699 <https://doi.org/10.1038/nclimate1744>, 2013.

700 Vigerstol, K. L. and Aukema, J. E.: A comparison of tools for modeling freshwater ecosystem services, *J. Environ.*
701 *Manage.*, 92, 2403–2409, <https://doi.org/10.1016/j.jenvman.2011.06.040>, 2011.

702 Villa, F., Bagstad, K., and Balbi, S.: ARIES: Artificial Intelligence for Environment & Sustainability, 2021.

703 Wheaton, E., Kulshreshtha, S., Wittrock, V., and Koshida, G.: Dry times: Hard lessons from the Canadian drought of
704 2001 and 2002, *Can. Geogr.*, 52, 241–262, <https://doi.org/10.1111/j.1541-0064.2008.00211.x>, 2008.

705 Wichelns, D.: Do estimates of water productivity enhance understanding of farm-level water management?, *Water*
706 (Switzerland), 6, 778–795, <https://doi.org/10.3390/w6040778>, 2014.

707 Xu, C., Li, Y., Hu, J., Yang, X., Sheng, S., and Liu, M.: Evaluating the difference between the normalized difference
708 vegetation index and net primary productivity as the indicators of vegetation vigor assessment at landscape scale,
709 *Environ. Monit. Assess.*, 184, 1275–1286, <https://doi.org/10.1007/s10661-011-2039-1>, 2012.

710 Xu, M., An, T., Zheng, Z., Zhang, T., Zhang, Y., and Yu, G.: Variability in evapotranspiration shifts from
711 meteorological to biological control under wet versus drought conditions in an alpine meadow, *J. Plant Ecol.*, 15, 921–
712 932, <https://doi.org/10.1093/jpe/rtac033>, 2022.

713 Xu, S., Frey, S. K., Erler, A. R., Khader, O., Berg, S. J., Hwang, H. T., Callaghan, M. V., Davison, J. H., and Sudicky,
714 E. A.: Investigating groundwater-lake interactions in the Laurentian Great Lakes with a fully-integrated surface water-
715 groundwater model, *J. Hydrol.*, 594, 125911, <https://doi.org/10.1016/j.jhydrol.2020.125911>, 2021.

716 Xu, Y. and Xiao, F.: Assessing Changes in the Value of Forest Ecosystem Services in Response to Climate Change
717 in China, *Sustain.*, 14, <https://doi.org/10.3390/su14084773>, 2022.

718 Xue, K., Song, L., Xu, Y., Liu, S., Zhao, G., Tao, S., Magliulo, E., Manco, A., Liddell, M., Wohlfahrt, G., Varlagin,
719 A., Montagnani, L., Woodgate, W., Loubet, B., and Zhao, L.: Estimating ecosystem evaporation and transpiration
720 using a soil moisture coupled two-source energy balance model across FLUXNET sites, *Agric. For. Meteorol.*, 337,
721 1–7, <https://doi.org/10.1016/j.agrformet.2023.109513>, 2023.

722 Yang, H., Luo, P., Wang, J., Mou, C., Mo, L., Wang, Z., Fu, Y., Lin, H., Yang, Y., and Bhatta, L. D.: Ecosystem
723 evapotranspiration as a response to climate and vegetation coverage changes in Northwest Yunnan, China, *PLoS One*,
724 10, 1–17, <https://doi.org/10.1371/journal.pone.0134795>, 2015.

725 Yang, X. and Liu, J.: Assessment and valuation of groundwater ecosystem services: A case study of Handan City,
726 China, *Water (Switzerland)*, 12, <https://doi.org/10.3390/w12051455>, 2020.

727 Yu, S., Miao, C., Song, H., Huang, Y., and Chen, W.: Efficiency of nitrogen and phosphorus removal by six
728 macrophytes from eutrophic water Efficiency of nitrogen and phosphorus removal by six macrophytes from eutrophic
729 water, *Int. J. Phytoremediation*, 21, 643–651, <https://doi.org/10.1080/15226514.2018.1556582>, 2019.

730 Zhang, T., Xu, M., Zhang, Y., Zhao, T., An, T., Li, Y., Sun, Y., Chen, N., Zhao, T., Zhu, J., and Yu, G.: Grazing-
731 induced increases in soil moisture maintain higher productivity during droughts in alpine meadows on the Tibetan
732 Plateau, *Agric. For. Meteorol.*, 269–270, 249–256, <https://doi.org/10.1016/j.agrformet.2019.02.022>, 2019.

733 Zhao, M., Aa, G., Liu, Y., and Konings, A.: Evapotranspiration frequently increases during droughts, *Nat. Clim.*
734 *Chang.*, 6904, 2022.

735 Zisopoulou, K., Zisopoulos, D., and Panagoulia, D.: Water Economics: An In-Depth Analysis of the Connection of
736 Blue Water with Some Primary Level Aspects of Economic Theory I, *Water (Switzerland)*, 14,
737 <https://doi.org/10.3390/w14010103>, 2022.

738

739 **Appendix**

740 The annual outputs (ET_a , surface water, subsurface water, precipitation and outflow) from the HGS model are given
741 in Table 1A.

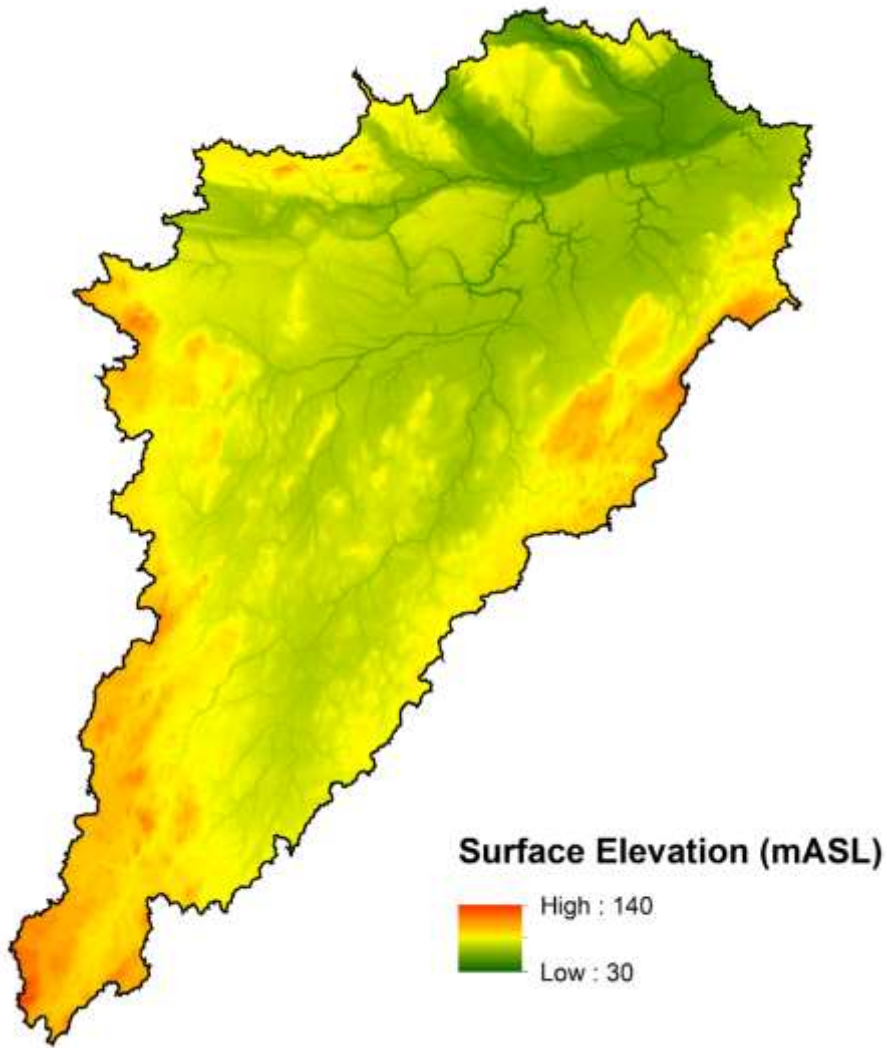
Table A1: HGS outputs from the SNW simulation

Year	ET_a (m³)	Surface water (m³)	Subsurface water (m³)	Precipitati on (m³)	Outflo w (m³)	Surfac e evapor ation (m³)	Subsur face evapor ation (m³)	Subsurf ace transpir ation (m³)
2000	2,085,53 4,445	69,424,628	222,709,069,4 60	4,199,527, 096	76,327, 719	75,020, 473	184,37 4,990	945,999, 818
2001	2,477,00 4,097	54,513,422	222,240,461,9 50	3,003,497, 233	32,382, 847	49,049, 150	193,68 4,126	1,525,26 3,969
2002	2,309,98 4,877	61,588,887	222,788,771,4 12	3,598,706, 939	50,743, 315	49,496, 381	137,24 6,184	150,943 1,700
2003	2,264,69 6,091	68,998,342	222,524,086,3 05	4,253,877, 105	64,623, 628	63,041, 934	155,34 5,628	1,263,07 3,935
2004	2,197,97 4,479	67,358,376	222,569,571,6 66	3,631,932, 688	47,291, 949	56,472, 059	186,21 7,551	1,224,54 5,264
2005	2,416,95 8,064	67,153,617	222,566,818,8 92	3,988,298, 138	48,434, 304	62,293, 999	203,74 5,742	1407,71 8,083
2006	2,293,95 0,204	74,422,486	222,666,754,3 61	4,538,849, 536	77,813, 027	73,310, 604	176,40 6,194	1,175,39 0,417
2007	2,385,26 0,383	65,967,543	222,611,557,1 49	3,679,748, 277	47,306, 909	55,442, 956	193,05 4,015	1,352,24 7,667
2008	2,236,13 9,918	79,130,070	222,736,726,6 08	5,070,858, 236	75,918, 796	63,243, 999	153,50 5,172	1,001,91 2,242
2009	2,142,95 6,266	72,673,133	222,733,824,1 27	3,753,041, 839	73,573, 865	74,320, 182	175,80 8,767	1,034,71 8,786
2010	2,450,48 0,102	67,043,193	222,626,541,1 97	3,686,832, 140	67,076, 288	78,166, 506	204,92 8,373	1,337,19 4,629
2011	2,398,27 5,129	63,710,702	222,487,837,8 13	3,743,641, 761	47,912, 738	56,432, 877	170,45 9,783	1,404,94 3,119

2012	2,589,09	52,013,667	222,334,569,7	2,864,258,	26,234,	58,974,	223,34	1,633,46
	4,745		69	811	849	276	8,145	5,101
2013	2,269,22	64,978,113	222,458,625,7	3,700,833,	54,270,	67,961,	205,25	1,227,71
	8,484		10	331	475	698	3,614	2,022
2014	2,193,04	69,944,514	222,574,462,5	3,974,971,	44,803,	67,115,	170,74	1,220,17
	1,030		08	693	342	318	0,982	9,455
2015	2,449,70	62,201,787	222,466,595,8	3,374,434,	14,781,	64,640,	227,93	1,407,05
	2,370		16	139	188	268	7,634	2,424
2016	2,516,78	59,120,794	222,402,665,8	3,747,4429	40,697,	53,448,	220,31	1,610,08
	0,613		68	09	558	526	3,313	7,162
2017	2,273,90	80,775,412	222,688,809,4	5,228,987,	63,739,	77,841,	192,36	1,176,49
	3,311		35	865	372	432	9,477	7,385

745

The SNW has approximately 110 m of vertical relief from its highest point in the southwest corner to its outlet at the Ottawa River at its northern edge (Fig. 1A).



750 Figure 1A: Land surface elevation of the SNW (Ontario Integrated Hydrology Data).

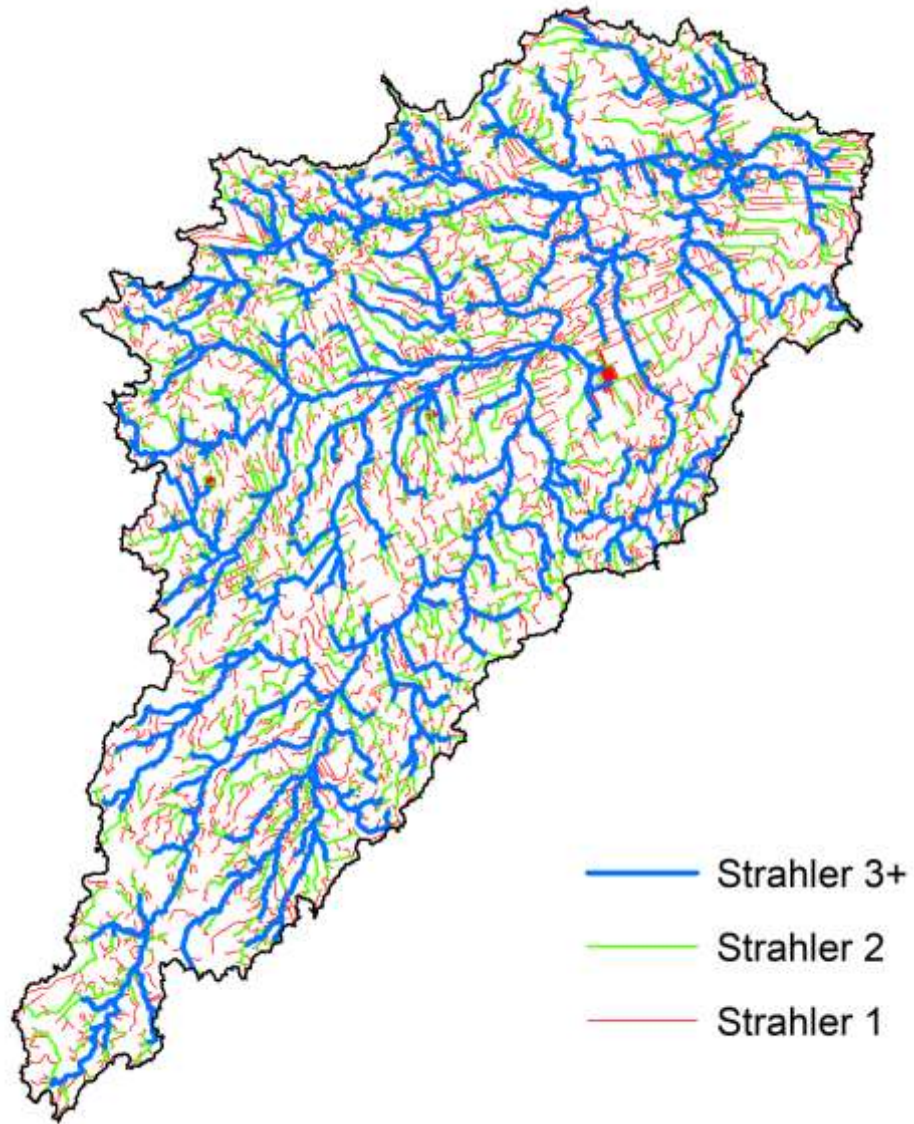
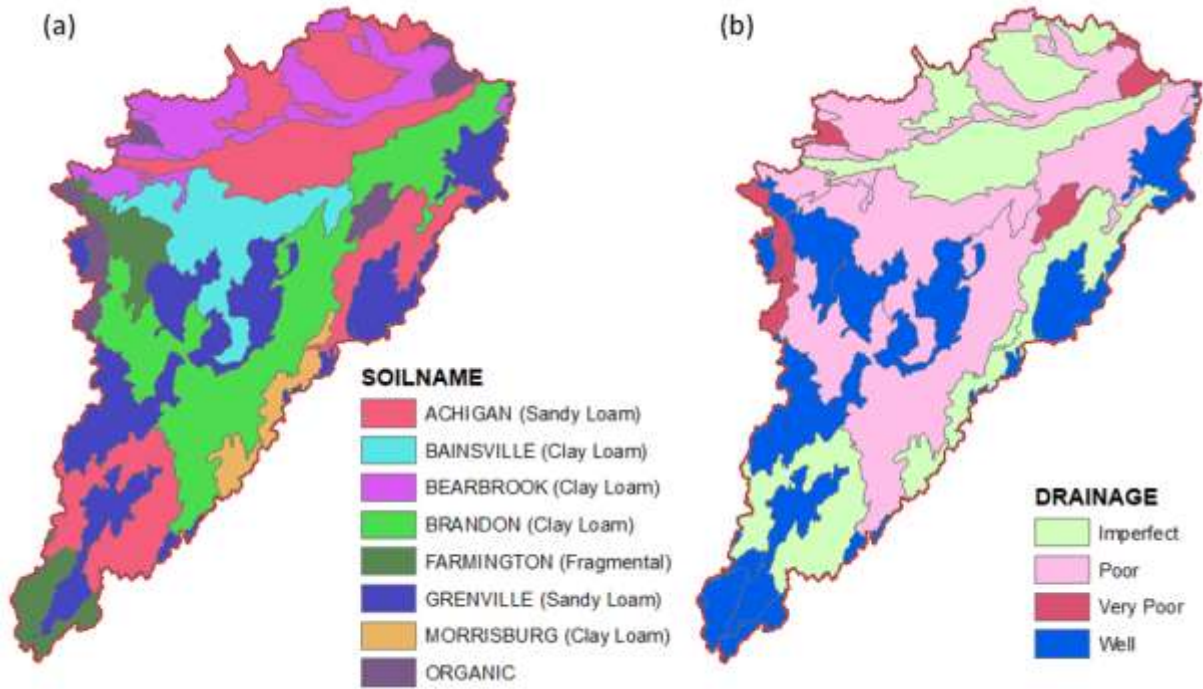


Figure 2A. Stream network distribution across the South Nation watershed, consisting of 1606 km of Strahler 3+ streams, 1548 km of Strahler 2 streams, and 3335 km of Strahler 1 streams (Ontario Ministry of Natural Resources and Forestry 2013).



755

Figure 3A. (a) Soil distribution, and (b) soil drainage status across the South Nation watershed (SLC, 2010) .

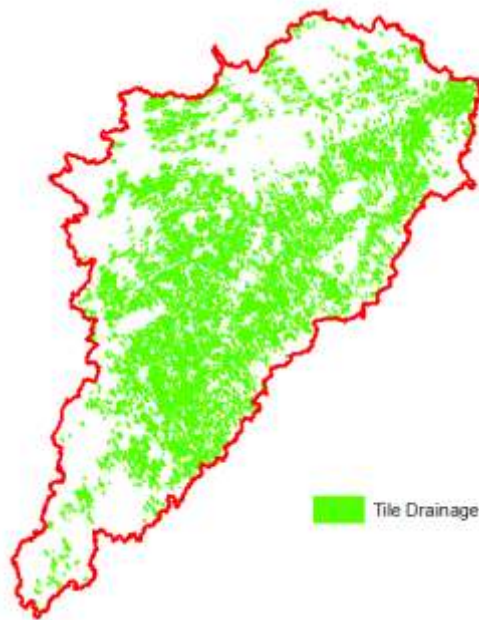
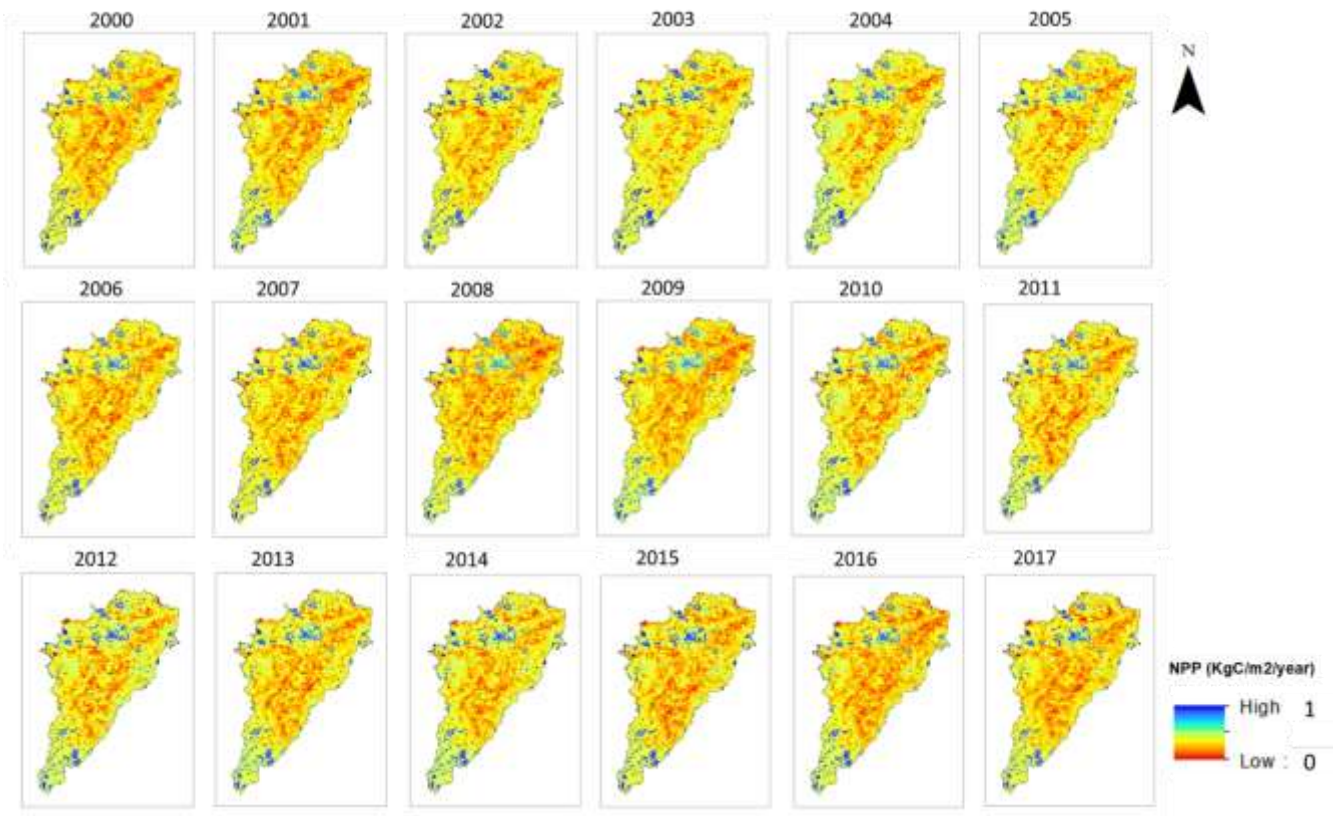


Figure 4A. Tile drainage distribution across the South Nation watershed (data provided by the South Nation Conservation Authority).



760

Figure 5A: Net Primary Productivity (NPP) data for SNW (based on MODIS data (Endsley et al., 2023))